Robust Decentralized Control of Inter-constrained Continuous Nonlinear Systems

A Receding Horizon Approach

ALEXANDROS FILOTHEOU

KTH Electrical Engineering

Master's Degree Project

Stockholm, Sweden February 2006

TRITA-EE 2006:666

Contents

Part I

Simulations

1

Introduction

The present part illustrates the efficacy of the advocated solutions, as described in chapters **??** and **??**, with regard to stabilization of multiple interconstrained agents, under the absence or presence of additive disturbances in chapters 2 and 3 respectively.

The benefit of solving the problem this thesis addresses, as was formulated in chapter **??** and approached in chapters **??** and **??**, is that the procured solutions can be applied to a general class of likewise problems − the similarity relation relates to/the terms, the dynamic nature of the actors, and the structure of their habitat, but not the spirit of the problem itself.

1.1 The operational model

The simulacrum used for all agents in the following chapters shall be the three-dimensional model of the unicycle; its motion shall be expressed by the nonlinear continuous-time kinematic equations

$$\dot{x} = v\cos\theta$$
$$\dot{y} = v\sin\theta$$
$$\dot{\theta} = \omega \tag{1.1}$$

with $\mathbf{z} = [x, y, \theta]^\top$ the vector of states, $\mathbf{u} = [v, \omega]^\top$ the vector of inputs, and $\dot{\mathbf{z}} = f(\mathbf{z}, \mathbf{u})$ the (model) system's equation. We consider that $\mathbf{x} \in X$, $\mathbf{y} \in Y$ where $X \equiv Y \equiv \mathbb{R}$, $\theta \in \Theta \equiv (-\pi, \pi]$ and $\mathbf{u} \in \mathcal{U}$. In this 2D spatial environment, the obstacles of the workspace along with the workspace boundary itself assume an appropriately reformed form: that of a circle. The labeled space in which an arbitrary agent i moves, along with the spherical-obstacles-transformed to circles, is depicted in figure (1.1).

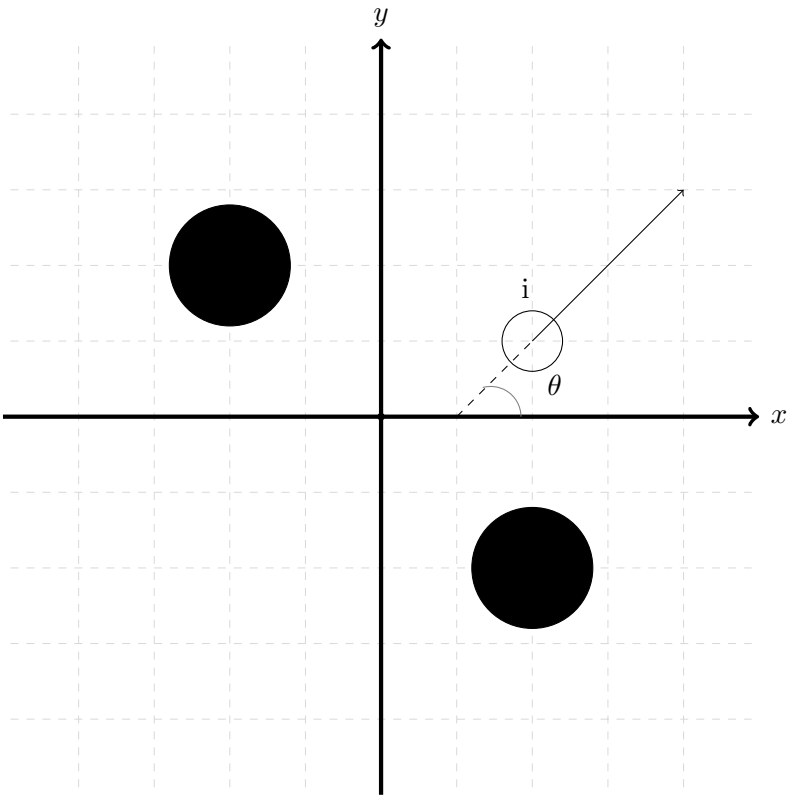

Figure 1.1: The 2D plane, agent i, whose orientation relative to the x axis is θ, and two obstacles.

The desired configuration shall be denoted by $\mathbf{z}_{des}$, the error dynamics by $\dot{\mathbf{e}} = g(\mathbf{e}, \mathbf{u})$ where $\mathbf{e}(t) = \mathbf{z}(t) - \mathbf{z}_{des}$ and $\mathbf{e} \in \mathcal{E} \equiv X \times Y \times \Theta \ominus \mathbf{z}_{des}$.

Lemma 1.1.1. Function g is Lipschitz continuous in $\mathcal{E} \times \mathcal{U}$ with a Lipschitz constant

$$L_g = v\sqrt{Q_{1,1} + Q_{1,2} + Q_{2,1} + Q_{2,2}}$$

where $\boldsymbol{Q} = Q_{\mu\nu}$ is the 3×3 matrix used to weigh the norms involved.

1.2 The problem reformed

Considering the conditions of the motivational problem as stated by problem (**??**), the reformed problem assumes the following form:

Problem 1.2.1. Assuming that

- all agents $i \in \mathcal{V}$ have access to their own and their neighbours' state and input vectors
- all agents $i \in \mathcal{V}$ have a (upper-bounded) sensing range d_i such that

$$d_i > \max\{r_i + r_j : \forall i, j \in \mathcal{V}, i \neq j\}$$

- at time $t = 0$ the sets $\mathcal{N}_i$ are known for all $i \in \mathcal{V}$ and $\sum_i |\mathcal{N}_i| > 0$
- at time $t = 0$ all agents are in a collision-free configuration with each other and the obstacles $\ell \in \mathcal{L}$
- All obstacles $\ell \in \mathcal{L}$ are situated in such a way that the distance between the two least distant obstacles is larger than the diameter of the agent with the largest diameter

the problem lies in procuring feasible controls for each agent $i \in \mathcal{V}$ such that for all agents and for all obstacles $\ell \in \mathcal{L}$ the following hold

1. Position and orientation configuration is achieved in steady-state $\mathbf{z}_{i,des}$

$$\lim_{t\to\infty} \|\mathbf{z}_i(t) - \mathbf{z}_{i,des}\| = 0$$

2. Inter-agent collision is avoided

$$\|\mathbf{p}_i(t) - \mathbf{p}_j(t)\| = d_{ij,a}(t) > \underline{d}_{ij,a}, \forall j \in \mathcal{V}\backslash\{i\}$$

where $\mathbf{p}(t) = [x(t), y(t)]^\top$

3. Inter-agent connectivity loss between neighbouring agents is avoided

$$\|\mathbf{p}_i(t) - \mathbf{p}_j(t)\| = d_{ij,a}(t) < d_i, \forall j \in \mathcal{N}_i, \forall i : |\mathcal{N}_i| \neq 0$$

4. Agent-with-obstacle collision is avoided

$$\|\mathbf{p}_i(t) - \mathbf{p}_\ell(t)\| = d_{i\ell,o}(t) > \underline{d}_{i\ell,o}, \forall \ell \in \mathcal{L}$$

5. The control laws $\mathbf{u}_i(t)$ abide by their respective input constraints

$$\mathbf{u}_i(t) \in \mathcal{U}_i$$

for appropriate choice of constants $r_i, \mathbf{z}_{i,des}, \underline{d}_{ij,a}, d_i, \underline{d}_{i\ell,o}$ and neighbour sets $\mathcal{N}_i$, where $i \in \mathcal{V}$.

From the above we conclude that the constraint set $\mathcal{Z}_i$ for agent $i \in \mathcal{V}$ is

$$\begin{aligned}\mathcal{Z}_{i,t} = \big\{\mathbf{z}_i(t) \in X \times Y \times \Theta : \|\mathbf{p}_i(t) - \mathbf{p}_j(t)\| > \underline{d}_{ij,a}, \forall j \in \mathcal{R}_i(t),\\ \|\mathbf{p}_i(t) - \mathbf{p}_j(t)\| < d_i, \forall j \in \mathcal{N}_i,\\ \|\mathbf{p}_i(t) - \mathbf{p}_\ell\| > \underline{d}_{i\ell,o}, \forall \ell \in \mathcal{L},\\ -\pi < \theta_i(t) \leq \pi\big\}\end{aligned}$$

and the constraint set that corresponds to each agent for all $i \in \mathcal{V}$ is given by the Minkowski difference

$$\mathcal{E}_{i,t} = \mathcal{Z}_{i,t} \ominus \mathbf{z}_{i,des} \tag{1.2}$$

The content of chapters 2 and 3 will demonstrate that agents $i \in \mathcal{V}$ can be stabilized when disturbances are absent, as demonstrated in chapter **??**, and, in the case where disturbances are present, that the magnitude of their errors about the equilibrium does not exceed a certain ceiling, as demonstrated in chapter **??**.

1.3 Simulation scenarios

The simulations shall be carried out under four different agents-obstacles configurations:

1. Two agents will have to avoid one obstacle on their way to their steady-state configurations, without colliding with each other and without being separated by the obstacle (we demand that their distance is always smaller than the obstacle's diameter for the sake of cooperation).

2. Two agents will have to pass through the space between two obstacles on their way to their steady-state configurations − again, the maximum allowed distance between the two agents is smaller than the diameter of the obstacle with the smallest diameter.

3. Three agents will have to avoid one obstacle on their way to their steady-state configurations, without colliding with each other and without being separated by the obstacle. In this case, two agents are (independently) neighbours of the third, that is, the third agent should maintain connectivity and avoid collision with both of the other two, but the latter will only have to avoid colliding with each other.

4. Three agents will have to pass through the space between two obstacles on their way to their steady-state configurations. The conditions of this scenario assume those of points 2 and 3.

The four configurations are depicted in figures (1.2), (1.3), (1.4) and (1.5). Agent 1 shall be depicted in blue, agent 2 in red and agent 3 in yellow. The obstacles shall be depicted in black. Mark X denotes the desired position of an agent and its colour signifies the agent to be stabilized in that position.

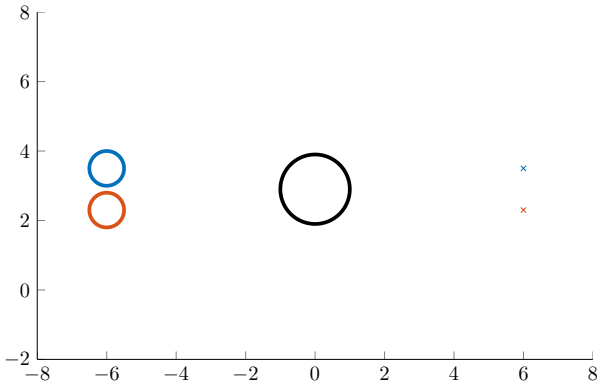

Figure 1.2: Test case one: two agents and one obstacle.

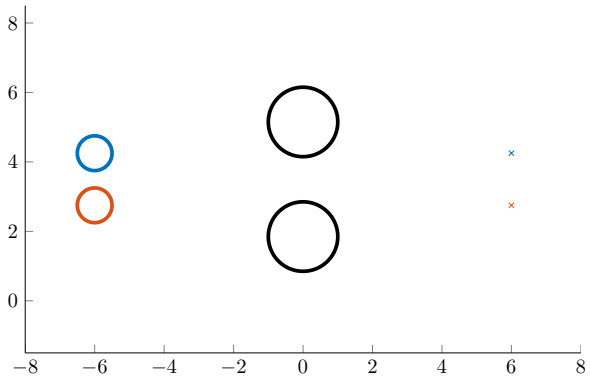

Figure 1.3: Test case two: two agents and two obstacles.

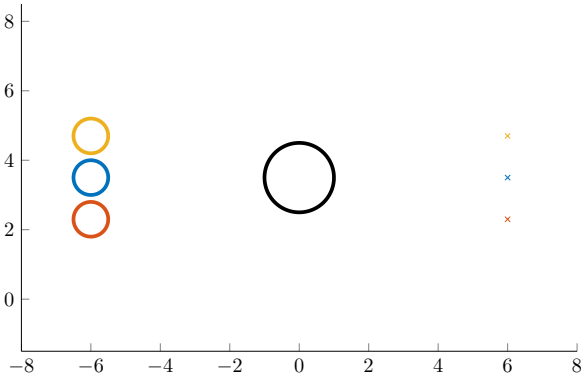

Figure 1.4: Test case three: three agents and one obstacle.

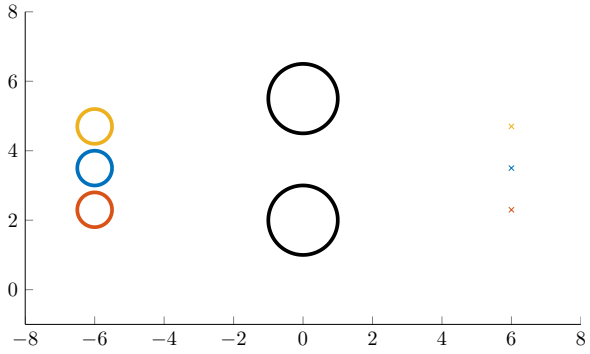

Figure 1.5: Test case four: three agents and two obstacles.

All configurations are as follows: the radius of all agents $i, j \in \mathcal{V}$ is $r_i = 0.5$; the radius of all obstacles is $r_\ell = 1.0$; the sensing range of all agents has a radius of $d_i = 4r_i + \epsilon = 2.0 + \epsilon$; the minimum distance between agents is $\underline{d}_{ij,a} = 2r_i + \epsilon = 1 + \epsilon$, and the minimum distance between agents and obstacles is $\underline{d}_{i\ell,o} = r_i + r_\ell + \epsilon = 1.5 + \epsilon$. ϵ was set to $\epsilon = 0.1$ in the disturbance-free cases and $\epsilon = 0.01$ in the cases where disturbances are present.

In the case of two agents, the neighbouring sets are $\mathcal{N}_1 = \{2\}$ and $\mathcal{N}_2 = \{1\}$, while in the case of three agents, $\mathcal{N}_1 = \{2, 3\}$, $\mathcal{N}_2 = \{1\}$ and $\mathcal{N}_3 = \{1\}$.

Under the above configuration regime, all agents are constrained in bypassing the obstacle(s) from the same side, as they are prohibited from overtaking it (them) from different sides by the requirement that their sensing range be lower than the sum of the diameter of one obstacle and the radii of any two agents.

The individual initial and terminal configurations of each agent, the positions of the obstacles and various other parameters shall be reported in the appropriate sections.

2

Simulations of Disturbance-free Stabililization

The present chapter illustrates the stabilization of a group of agents whose motion dynamics are expressed by equations (1.1), and whose errors with respect to their respective steady-state configurations are constrained by the set found in equation (1.2).

Each of the following sections describes the initial and terminal configurations, and the penalty matrices $\boldsymbol{Q}$, $\boldsymbol{R}$ and $\boldsymbol{P}$ used in each setting. Furthermore, the errors of each agent with respect to its terminal configuration are portrayed, along with its inputs signals and the distances between all agents and obstacles. Boundary values for the aforementioned inputs and distances shall be portrayed in the colour cyan. All simulations were performed with a sampling time of $h = 0.1$ sec, a time-horizon of $T_p = 0.5$ sec; the total execution time given was 3 sec.

3

Simulations of Stabilization in the face of Disturbances

For compatibility with real situations, we assume that in the case of disturbances, the signals affecting the agents are of the same nature (consider for instance the case of UAV's affected by wind); the disturbance signal considered was $\delta(t) = 0.1 * \sin 2t$. Therefore, $\overline{\delta} = 0.1$

Appendices

A

Proofs of lemmas

A.1 Proof of lemma 0

Let $\lambda_{min}(\boldsymbol{Q}_i, \boldsymbol{R}_i)$ denote the smallest eigenvalue between those of matrices $\boldsymbol{Q}_i$ and $\boldsymbol{R}_i$, and let $\lambda_{max}(\boldsymbol{Q}_i, \boldsymbol{R}_i)$ denote the largest. Then

$$\lambda_{min}(\boldsymbol{Q}_i, \boldsymbol{R}_i)\|\mathbf{e}_i(t)\|^2 \leq \lambda_{min}(\boldsymbol{Q}_i, \boldsymbol{R}_i)\left\| \begin{bmatrix} \mathbf{e}_i(t) \\ \mathbf{u}_i(t) \end{bmatrix} \right\|^2$$

$$\leq F_i\big(\mathbf{e}_i(t), \mathbf{u}_i(t)\big)$$

$$\leq \lambda_{max}(\boldsymbol{Q}_i, \boldsymbol{R}_i)\left\| \begin{bmatrix} \mathbf{e}_i(t) \\ \mathbf{u}_i(t) \end{bmatrix} \right\|^2 \leq \lambda_{max}(\boldsymbol{Q}_i, \boldsymbol{R}_i)\|\mathbf{e}_i(t)\|^2$$

Matrices $\boldsymbol{Q}_i, \boldsymbol{R}_i$ are positive definite, hence the functions $\alpha_1\big(\|\mathbf{e}_i\|\big) = \lambda_{min}(\boldsymbol{Q}_i, \boldsymbol{R}_i)\|\mathbf{e}_i\|^2$ and $\alpha_2\big(\|\mathbf{e}_i\|\big) = \lambda_{max}(\boldsymbol{Q}_i, \boldsymbol{R}_i)\|\mathbf{e}_i\|^2$ are class $\mathcal{K}_\infty$ functions according to definition (**??**). Therefore, F_i is lower- and upper-bounded by class $\mathcal{K}_\infty$ functions:

$$\alpha_1\big(\|\mathbf{e}_i\|\big) \leq F_i\big(\mathbf{e}_i, \mathbf{u}_i\big) \leq \alpha_2\big(\|\mathbf{e}_i\|\big)$$

A.2 Proof of lemma 0

For every $\mathbf{e}_1, \mathbf{e}_2 \in \mathcal{E}_i$, and $\mathbf{u}_i \in \mathcal{U}_i$ it holds that

$$\begin{aligned}
\big|F_i(\mathbf{e}_1, \mathbf{u}_i) - F_i(\mathbf{e}_2, \mathbf{u}_i)\big| &= \big|\mathbf{e}_1^\top \boldsymbol{Q}_i \mathbf{e}_1 + \mathbf{u}_i^\top \boldsymbol{R}_i \mathbf{u}_i - \mathbf{e}_2^\top \boldsymbol{Q}_i \mathbf{e}_2 - \mathbf{u}_i^\top \boldsymbol{R}_i \mathbf{u}_i\big| \\
&= \big|\mathbf{e}_1^\top \boldsymbol{Q}_i \mathbf{e}_1 - \mathbf{e}_2^\top \boldsymbol{Q}_i \mathbf{e}_2 \pm \mathbf{e}_1^\top \boldsymbol{Q}_i \mathbf{e}_2\big| \\
&= \big|\mathbf{e}_1^\top \boldsymbol{Q}_i (\mathbf{e}_1 - \mathbf{e}_2) - \mathbf{e}_2^\top \boldsymbol{Q}_i (\mathbf{e}_1 - \mathbf{e}_2)\big| \\
&\leq \big|\mathbf{e}_1^\top \boldsymbol{Q}_i (\mathbf{e}_1 - \mathbf{e}_2)\big| + \big|\mathbf{e}_2^\top \boldsymbol{Q}_i (\mathbf{e}_1 - \mathbf{e}_2)\big|
\end{aligned}$$

But for any $\mathbf{e}_1, \mathbf{e}_2 \in \mathcal{E}_i$

$$|\mathbf{e}_1^\top \boldsymbol{Q}_i \mathbf{e}_2| \leq \sigma_{max}(\boldsymbol{Q}_i)\|\mathbf{e}_1\|\|\mathbf{e}_2\|$$

where $\sigma_{max}(\boldsymbol{Q}_i)$ denotes the largest singular value of matrix $\boldsymbol{Q}_i$. Hence:

$$\begin{aligned}
\big|F_i(\mathbf{e}_1, \mathbf{u}_i) - F_i(\mathbf{e}_2, \mathbf{u}_i)\big| &\leq \sigma_{max}(\boldsymbol{Q}_i)\|\mathbf{e}_1\|\|\mathbf{e}_1 - \mathbf{e}_2\| + \sigma_{max}(\boldsymbol{Q}_i)\|\mathbf{e}_2\|\|\mathbf{e}_1 - \mathbf{e}_2\| \\
&= \sigma_{max}(\boldsymbol{Q}_i)(\|\mathbf{e}_1\| + \|\mathbf{e}_2\|)\|\mathbf{e}_1 - \mathbf{e}_2\| \\
&= \sigma_{max}(\boldsymbol{Q}_i) \sup_{\mathbf{e}_1, \mathbf{e}_2 \in \mathcal{E}_i} \big(\|\mathbf{e}_1\| + \|\mathbf{e}_2\|\big)\|\mathbf{e}_1 - \mathbf{e}_2\| \\
&= 2\sigma_{max}(\boldsymbol{Q}_i) \sup_{\mathbf{e}_i \in \mathcal{E}_i} \big(\|\mathbf{e}_i\|\big)\|\mathbf{e}_1 - \mathbf{e}_2\| \\
&= 2\sigma_{max}(\boldsymbol{Q}_i)\overline{\varepsilon}_i\|\mathbf{e}_1 - \mathbf{e}_2\|
\end{aligned}$$

A.3 Proof of lemma 0

For every $\mathbf{e}_1, \mathbf{e}_2 \in \Omega_i$, it holds that

$$\begin{aligned}
\big|V_i(\mathbf{e}_1) - V_i(\mathbf{e}_2)\big| &= \big|\mathbf{e}_1^\top \boldsymbol{P}_i \mathbf{e}_1 - \mathbf{e}_2^\top \boldsymbol{P}_i \mathbf{e}_2\big| \\
&= \big|\mathbf{e}_1^\top \boldsymbol{P}_i \mathbf{e}_1 - \mathbf{e}_2^\top \boldsymbol{P}_i \mathbf{e}_2 \pm \mathbf{e}_1^\top \boldsymbol{P}_i \mathbf{e}_2\big| \\
&= \big|\mathbf{e}_1^\top \boldsymbol{P}_i (\mathbf{e}_1 - \mathbf{e}_2) - \mathbf{e}_2^\top \boldsymbol{P}_i (\mathbf{e}_1 - \mathbf{e}_2)\big| \\
&\leq \big|\mathbf{e}_1^\top \boldsymbol{P}_i (\mathbf{e}_1 - \mathbf{e}_2)\big| + \big|\mathbf{e}_2^\top \boldsymbol{P}_i (\mathbf{e}_1 - \mathbf{e}_2)\big|
\end{aligned}$$

But for any $\mathbf{e}_1, \mathbf{e}_2 \in \mathbb{R}^n$

$$\big|\mathbf{e}_1^\top \boldsymbol{P}_i \mathbf{e}_2\big| \leq \sigma_{max}(\boldsymbol{P}_i)\|\mathbf{e}_1\|\|\mathbf{e}_2\|$$

where $\sigma_{max}(\boldsymbol{P}_i)$ denotes the largest singular value of matrix $\boldsymbol{P}_i$. Hence:

$$\begin{aligned}
\big|V_i(\mathbf{e}_1) - V_i(\mathbf{e}_2)\big| &\leq \sigma_{max}(\boldsymbol{P}_i)\|\mathbf{e}_1\|\|\mathbf{e}_1 - \mathbf{e}_2\| + \sigma_{max}(\boldsymbol{P}_i)\|\mathbf{e}_2\|\|\mathbf{e}_1 - \mathbf{e}_2\| \\
&= \sigma_{max}(\boldsymbol{P}_i)(\|\mathbf{e}_1\| + \|\mathbf{e}_2\|)\|\mathbf{e}_1 - \mathbf{e}_2\| \\
&\leq \sigma_{max}(\boldsymbol{P}_i)(\overline{\varepsilon}_{i,\Omega_i} + \overline{\varepsilon}_{i,\Omega_i})\|\mathbf{e}_1 - \mathbf{e}_2\| \\
&= 2\sigma_{max}(\boldsymbol{P}_i)\overline{\varepsilon}_{i,\Omega_i}\|\mathbf{e}_1 - \mathbf{e}_2\|
\end{aligned}$$

A.4 Proof of lemma 0

V_i is defined as $V_i\big(\mathbf{e}_i\big) = \mathbf{e}_i^\top \boldsymbol{P}_i \mathbf{e}_i$. Let us denote the minimum and maximum eigenvalues of matrix $\boldsymbol{P}_i$ by $\lambda_{min}(\boldsymbol{P}_i)$ and $\lambda_{max}(\boldsymbol{P}_i)$ respectively. Then, the following series of inequalities holds:

$$\lambda_{min}(\boldsymbol{P}_i)\|\mathbf{e}_i\|^2 \leq V_i(\mathbf{e}_i) \leq \lambda_{max}(\boldsymbol{P}_i)\|\mathbf{e}_i\|^2$$

Matrix $\boldsymbol{P}_i$ is positive definite, hence the functions $\alpha_1 = \lambda_{min}(\boldsymbol{P}_i)\|\mathbf{e}_i\|^2$ and $\alpha_2 = \lambda_{max}(\boldsymbol{P}_i)\|\mathbf{e}_i\|^2$ are class $\mathcal{K}_\infty$ functions according to definition (**??**). Therefore, V_i is lower- and upper-bounded by class $\mathcal{K}_\infty$ functions:

$$\alpha_1\big(\|\mathbf{e}_i\|\big) \leq V_i(\mathbf{e}_i) \leq \alpha_2\big(\|\mathbf{e}_i\|\big)$$

A.5 Proof of property 0

Let us define for convenience $\boldsymbol{\zeta}_i : \mathbb{R}_{\geq 0} \to \mathbb{R}^9 \times \mathbb{T}^3$: $\boldsymbol{\zeta}_i(s) \triangleq \mathbf{e}_i(s) - \overline{\mathbf{e}}_i(s;\ \mathbf{u}_i(s;\ \mathbf{e}_i(t)), \mathbf{e}_i(t))$, for $s \in [t, t+T_p]$.

According to lemma (**??**)

$$\|\mathbf{e}_i(s) - \overline{\mathbf{e}}_i\big(s;\ \mathbf{u}_i(s;\ \mathbf{e}_i(t)), \mathbf{e}_i(t)\big)\| \leq \frac{\overline{\delta}_i}{\mathrm{L}_{g_i}}(e^{L_{g_i}(s-t)} - 1)$$

$$\|\boldsymbol{\zeta}_i(s)\| \leq \frac{\overline{\delta}_i}{\mathrm{L}_{g_i}}(e^{L_{g_i}(s-t)} - 1)$$

which means that $\boldsymbol{\zeta}_i(s) \in \mathcal{B}_{i,s-t}$. Now let us assume that $\overline{\mathbf{e}}_i\big(s;\ \mathbf{u}_i(\cdot,\ \mathbf{e}_i(t)), \mathbf{e}_i(t)\big) \in \mathcal{E}_i \ominus \mathcal{B}_{i,s-t}$. Then, we add the two include statements:

$$\overline{\mathbf{e}}_i\big(s;\ \mathbf{u}_i(\cdot,\ \mathbf{e}_i(t)), \mathbf{e}_i(t)\big) \in \mathcal{E}_i \ominus \mathcal{B}_{i,s-t}$$

$$\boldsymbol{\zeta}_i(s) \in \mathcal{B}_{i,s-t}$$

which yields

$$\boldsymbol{\zeta}_i(s) + \overline{\mathbf{e}}_i\big(s;\ \mathbf{u}_i(s;\ \mathbf{e}_i(t)), \mathbf{e}_i(t)\big) \in \big(\mathcal{E}_i \ominus \mathcal{B}_{i,s-t}\big) \oplus \mathcal{B}_{i,s-t}$$

Utilizing Theorem 2.1 (ii) from [**?**] yields

$$\boldsymbol{\zeta}_i(s) + \overline{\mathbf{e}}_i\big(s;\ \mathbf{u}_i(s;\ \mathbf{e}_i(t)), \mathbf{e}_i(t)\big) \in \mathcal{E}_i$$

$$\mathbf{e}_i(s) \in \mathcal{E}_i$$

A.6 Proof of lemma 0

Since there are disturbances present, consulting remark (**??**) and substituting for $\tau_0 = t$ and $\tau_1 = t + \tau$ yields:

$$\mathbf{e}_i\big(t+\tau;\ \overline{\mathbf{u}}_i^\star\big(\cdot;\ \mathbf{e}_i(t)\big), \mathbf{e}_i(t)\big) = \mathbf{e}_i(t) + \int_t^{t+\tau} g_i\big(\mathbf{e}_i(s;\ \mathbf{e}_i(t)), \overline{\mathbf{u}}_i^\star(s)\big)ds + \int_t^{t+\tau} \delta_i(s)ds$$

$$\overline{\mathbf{e}}_i\big(t+\tau;\ \overline{\mathbf{u}}_i^\star\big(\cdot;\ \mathbf{e}_i(t)\big), \mathbf{e}_i(t)\big) = \mathbf{e}_i(t) + \int_t^{t+\tau} g_i\big(\overline{\mathbf{e}}_i(s;\ \mathbf{e}_i(t)), \overline{\mathbf{u}}_i^\star(s)\big)ds$$

Subtracting the latter from the former and taking norms on either side yields:

$$\begin{aligned}
&\left\|\mathbf{e}_i\big(t+\tau;\ \overline{\mathbf{u}}_i^\star\big(\cdot;\ \mathbf{e}_i(t)\big), \mathbf{e}_i(t)\big) - \overline{\mathbf{e}}_i\big(t+\tau;\ \overline{\mathbf{u}}_i^\star\big(\cdot;\ \mathbf{e}_i(t)\big), \mathbf{e}_i(t)\big)\right\| \\
&\quad = \left\| \int_t^{t+\tau} g_i\big(\mathbf{e}_i(s;\ \mathbf{e}_i(t)), \overline{\mathbf{u}}_i^\star(s)\big)ds - \int_t^{t+\tau} g_i\big(\overline{\mathbf{e}}_i(s;\ \mathbf{e}_i(t)), \overline{\mathbf{u}}_i^\star(s)\big)ds + \int_t^{t+\tau} \delta_i(s)ds \right\| \\
&\quad \leq \left\| \int_t^{t+\tau} g_i\big(\mathbf{e}_i(s;\ \mathbf{e}_i(t)), \overline{\mathbf{u}}_i^\star(s)\big)ds - \int_t^{t+\tau} g_i\big(\overline{\mathbf{e}}_i(s;\ \mathbf{e}_i(t)), \overline{\mathbf{u}}_i^\star(s)\big)ds \right\| + (t+\tau-t)\overline{\delta}_i \\
&\quad = \int_t^{t+\tau} \left\| g_i\big(\mathbf{e}_i(s;\ \mathbf{e}_i(t)), \overline{\mathbf{u}}_i^\star(s)\big)s - g_i\big(\overline{\mathbf{e}}_i(s;\ \mathbf{e}_i(t)), \overline{\mathbf{u}}_i^\star(s)\big) \right\| ds + \tau\overline{\delta}_i \\
&\quad \leq L_{g_i} \int_t^{t+\tau} \left\| \mathbf{e}_i\big(s;\ \overline{\mathbf{u}}_i^\star\big(\cdot;\ \mathbf{e}_i(t)\big), \mathbf{e}_i(t)\big) - \overline{\mathbf{e}}_i\big(s;\ \overline{\mathbf{u}}_i^\star\big(\cdot;\ \mathbf{e}_i(t)\big), \mathbf{e}_i(t)\big) \right\| ds + \tau\overline{\delta}_i
\end{aligned}$$

since g_i is Lipschitz continuous in $\mathcal{E}_i$ with Lipschitz constant L_{g_i}. Reformulation yields

$$\begin{aligned}
&\left\|\mathbf{e}_i\big(t+\tau;\ \overline{\mathbf{u}}_i^\star\big(\cdot;\ \mathbf{e}_i(t)\big), \mathbf{e}_i(t)\big) - \overline{\mathbf{e}}_i\big(t+\tau;\ \overline{\mathbf{u}}_i^\star\big(\cdot;\ \mathbf{e}_i(t)\big), \mathbf{e}_i(t)\big)\right\| \\
&\qquad \leq \tau\overline{\delta}_i + L_{g_i} \int_0^{\tau} \left\| \mathbf{e}_i\big(t+s;\ \overline{\mathbf{u}}_i^\star\big(\cdot;\ \mathbf{e}_i(t)\big), \mathbf{e}_i(t)\big) - \overline{\mathbf{e}}_i\big(t+s;\ \overline{\mathbf{u}}_i^\star\big(\cdot;\ \mathbf{e}_i(t)\big), \mathbf{e}_i(t)\big) \right\| ds
\end{aligned}$$

By applying the Grönwall-Bellman inequality we get:

$$\begin{aligned}
&\Big\|\mathbf{e}_i\big(t+\tau;\ \overline{\mathbf{u}}_i^\star\big(\cdot;\ \mathbf{e}_i(t)\big),\mathbf{e}_i(t)\big) - \overline{\mathbf{e}}_i\big(t+\tau;\ \overline{\mathbf{u}}_i^\star\big(\cdot;\ \mathbf{e}_i(t)\big),\mathbf{e}_i(t)\big)\Big\| \\
&\qquad \leq \tau\overline{\delta}_i + L_{g_i}\int_0^\tau s\overline{\delta}_i e^{L_{g_i}(\tau-s)}ds \\
&\qquad = \tau\overline{\delta}_i - \overline{\delta}_i\int_0^\tau s\big(e^{L_{g_i}(\tau-s)}\big)'ds \\
&\qquad = \tau\overline{\delta}_i - \overline{\delta}_i\bigg(\big[se^{L_{g_i}(\tau-s)}\big]_0^\tau - \int_0^\tau e^{L_{g_i}(\tau-s)}ds\bigg) \\
&\qquad = \tau\overline{\delta}_i - \overline{\delta}_i\bigg(\tau + \frac{1}{L_{g_i}}(1-e^{L_{g_i}\tau})\bigg) \\
&\qquad = \frac{\overline{\delta}_i}{L_{g_i}}(e^{L_{g_i}\tau}-1)
\end{aligned}$$

A.7 Proof of lemma 1.1.1

Let $g(\mathbf{e},\mathbf{u})$ be the differential equation describing the error of the motion of the unicycle with respect to a fixed desired configuration, and $\boldsymbol{Q} = Q_{\mu\nu}$ a 3×3 matrix. Then

$$\begin{aligned}
\|g(\mathbf{e}_1,\mathbf{u}) - g(\mathbf{e}_2,\mathbf{u})\|_Q &= \left\| \begin{bmatrix} v\cos\theta_1 - v\cos\theta_2 \\ v\sin\theta_1 - v\sin\theta_2 \\ \omega-\omega \end{bmatrix} \right\|_Q \\
&= \sqrt{v^2\begin{bmatrix}\cos\theta_1-\cos\theta_2 & \sin\theta_1-\sin\theta_2 & 0\end{bmatrix} Q \begin{bmatrix}\cos\theta_1-\cos\theta_2 \\ \sin\theta_1-\sin\theta_2 \\ 0\end{bmatrix}} \\
&= \sqrt{v^2(\cos\theta_1-\cos\theta_2)\Big((Q_{11}+Q_{12})(\cos\theta_1-\cos\theta_2)+(Q_{21}+Q_{22})(\sin\theta_1-\sin\theta_2)\Big)}
\end{aligned}$$

From the mean value theorem we derive the following

$$\cos\theta_1 - \cos\theta_2 = -\sin\gamma(\theta_1-\theta_2) \leq |\theta_1-\theta_2|$$

$$\sin\theta_1 - \sin\theta_2 = \cos\gamma(\theta_1 - \theta_2) \leq |\theta_1 - \theta_2|$$

where $\theta_1 \leq \gamma \leq \theta_2$. Hence

$$\begin{aligned}
\|g(\mathbf{e}_1, \mathbf{u}) - g(\mathbf{e}_2, \mathbf{u})\|_Q &\leq \sqrt{v^2|\theta_1 - \theta_2|\Big((Q_{11} + Q_{12})|\theta_1 - \theta_2| + (Q_{21} + Q_{22})|\theta_1 - \theta_2|\Big)} \\
&= \sqrt{v^2|\theta_1 - \theta_2|^2(Q_{1,1} + Q_{1,2} + Q_{2,1} + Q_{2,2})} \\
&= v\sqrt{Q_{1,1} + Q_{1,2} + Q_{2,1} + Q_{2,2}} \cdot |\theta_1 - \theta_2|
\end{aligned}$$

B

Simulation figures – disturbances absent

B.1 Test case one: two agents – one obstacle

In this case the initial configurations of the two agents are $\mathbf{z}_1 = [-6, 3.5, 0]^\top$ and $\mathbf{z}_2 = [-6, 2.3, 0]^\top$. Their desired configurations in steady-state are $\mathbf{z}_{1,des} = [6, 3.5, 0]^\top$ and $\mathbf{z}_{2,des} = [6, 2.3, 0]^\top$. The obstacle is placed between the two, at $[0, 2.9]^\top$. The penalty matrices $\boldsymbol{Q}$, $\boldsymbol{R}$, $\boldsymbol{P}$ were set to $\boldsymbol{Q} = 0.5(I_3 + 0.1\dagger_3)$, $\boldsymbol{R} = 0.005I_2$ and $\boldsymbol{P} = 0.5I_3$, where $\dagger_N$ is a $N \times N$ matrix whose elements are chosen at random between the values 0.0 and 1.0.

In subsection 4.1.1, frames of the evolution of the trajectories of the two agents are depicted. Subsections 4.1.2 and 4.1.4 illustrate the evolution of the error states and the input signals of the two agents respectively. Subsection 4.1.3 features the figures relating to the evolution of the distance between the two agents along with that between them and the obstacle.

B.1.1 Trajectories in 2D

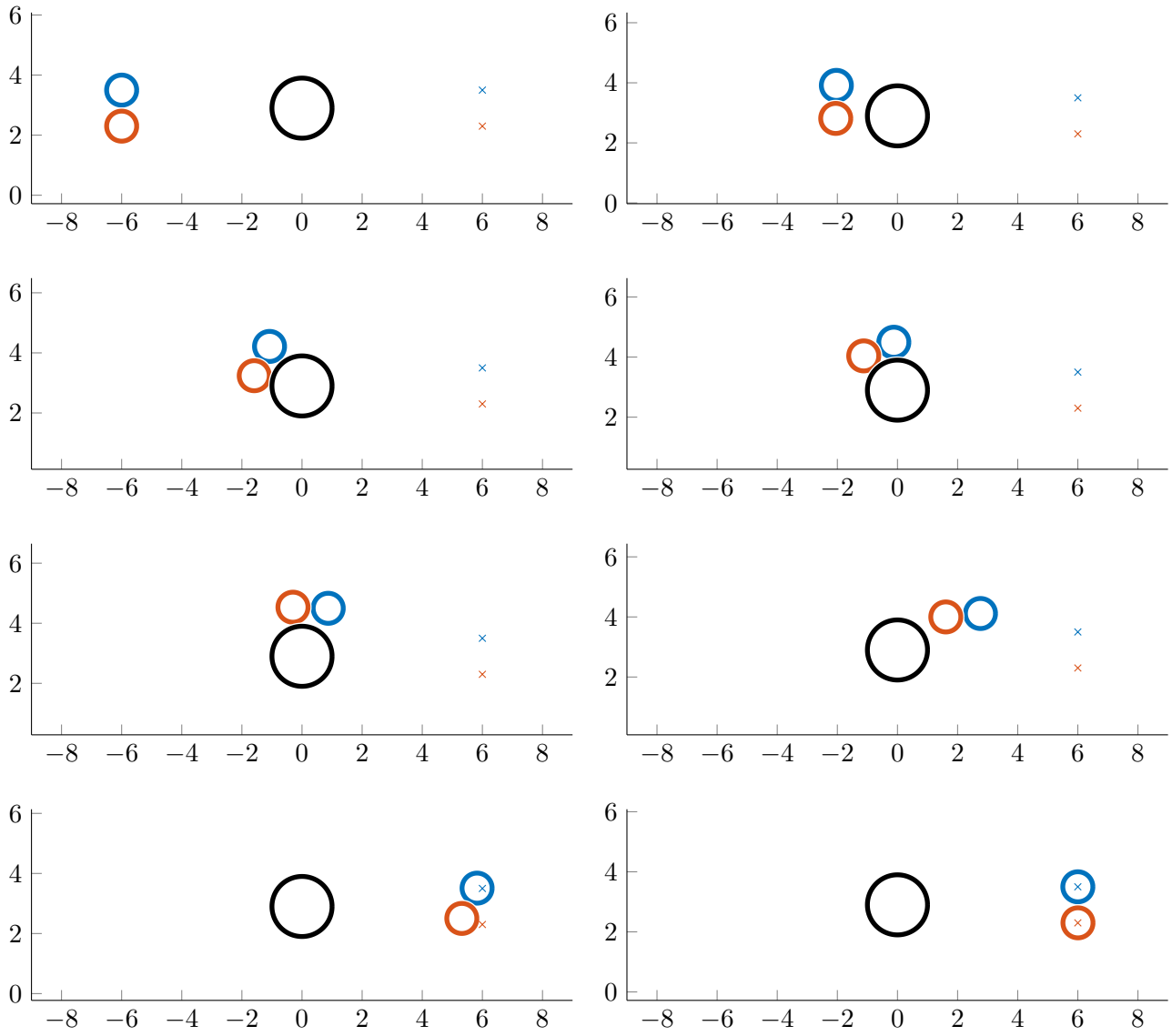

Figure B.1: The trajectories of the two agents in the $x - y$ plane.

B.1.2 State errors

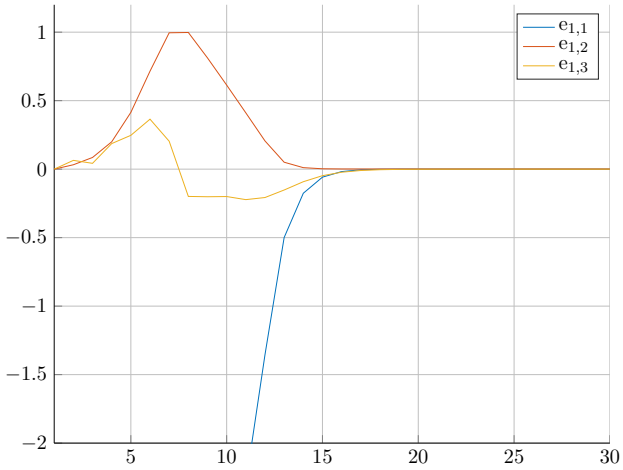

Figure B.2: The evolution of the error states of agent 1 over time.

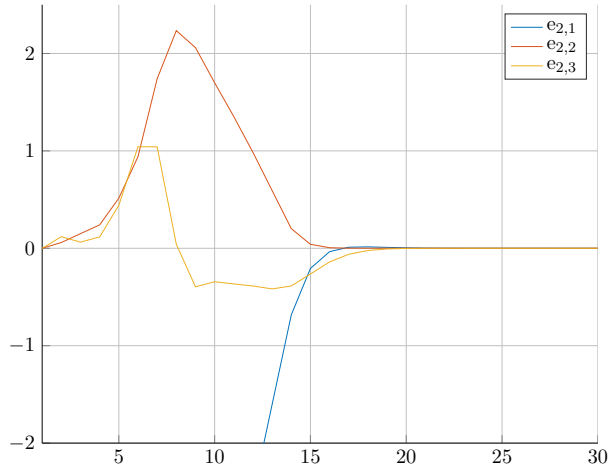

Figure B.3: The evolution of the error states of agent 2 over time.

B.1.3 Distances between actors

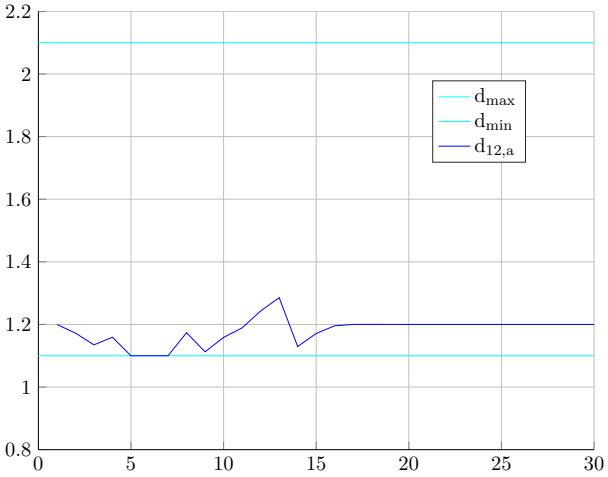

Figure B.4: The distance between the two agents over time. The maximum allowed distance has a value of 2.1 and the minimum allowed distance a value of 1.1.

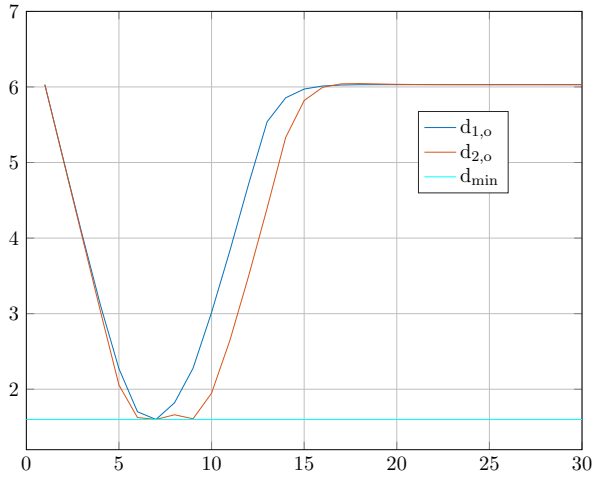

Figure B.5: The distance between each agent and the obstacle over time. The minimum allowed distance has a value of 1.6.

B.1.4 Input signals

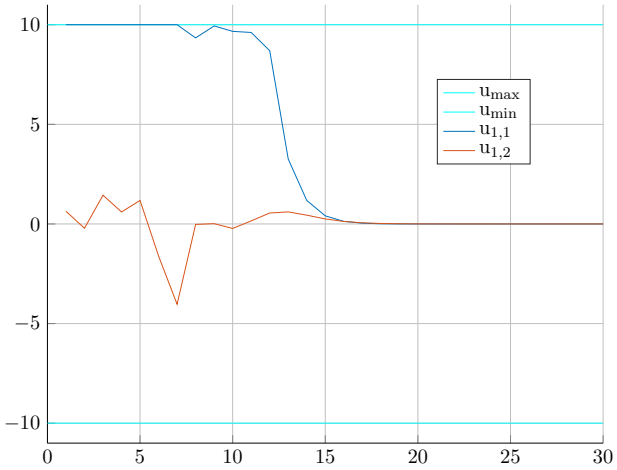

Figure B.6: The inputs signals directing agent 1 over time. Their value is constrained between −10 and 10.

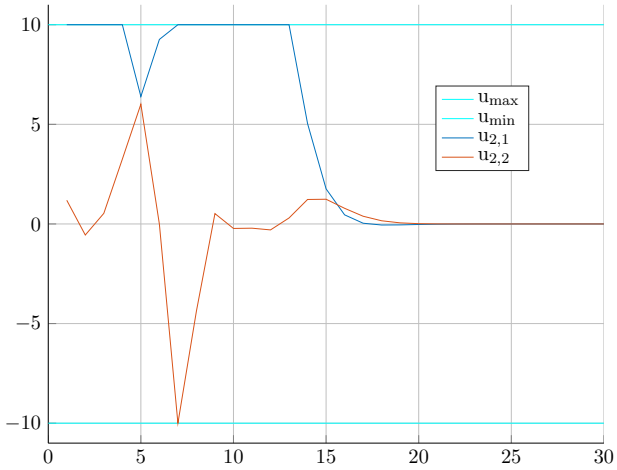

Figure B.7: The inputs signals directing agent 2 over time. Their value is constrained between −10 and 10.

B.2 Test case two: two agents – two obstacles

In this case the initial configurations of the two agents are $\mathbf{z}_1 = [-6, 2.75, 0]^\top$ and $\mathbf{z}_2 = [-6, 4.25, 0]^\top$. Their desired configurations in steady-state are $\mathbf{z}_{1,des} = [6, 2.75, 0]^\top$ and $\mathbf{z}_{2,des} = [6, 4.25, 0]^\top$. Obstacles o_1, 0_2 are placed between the two, at $[0, 1.85]^\top$ and $[0, 5.15]^\top$ respectively. The penalty matrices $\boldsymbol{Q}$, $\boldsymbol{R}$, $\boldsymbol{P}$ were set to $\boldsymbol{Q} = 0.5(I_3 + 0.1\dagger_3)$, $\boldsymbol{R} = 0.005I_2$ and $\boldsymbol{P} = 0.5I_3$, where $\dagger_N$ is a $N \times N$ matrix whose elements are chosen at random between the values 0.0 and 1.0.

In subsection 4.2.1, frames of the evolution of the trajectories of the two agents are depicted. Subsections 4.2.2 and 4.2.4 illustrate the evolution of the error states and the input signals of the two agents respectively. Subsection 4.2.3 features the figures relating to the evolution of the distance between the two agents along with that between them and the two obstacles.

B.2.1 Trajectories in 2D

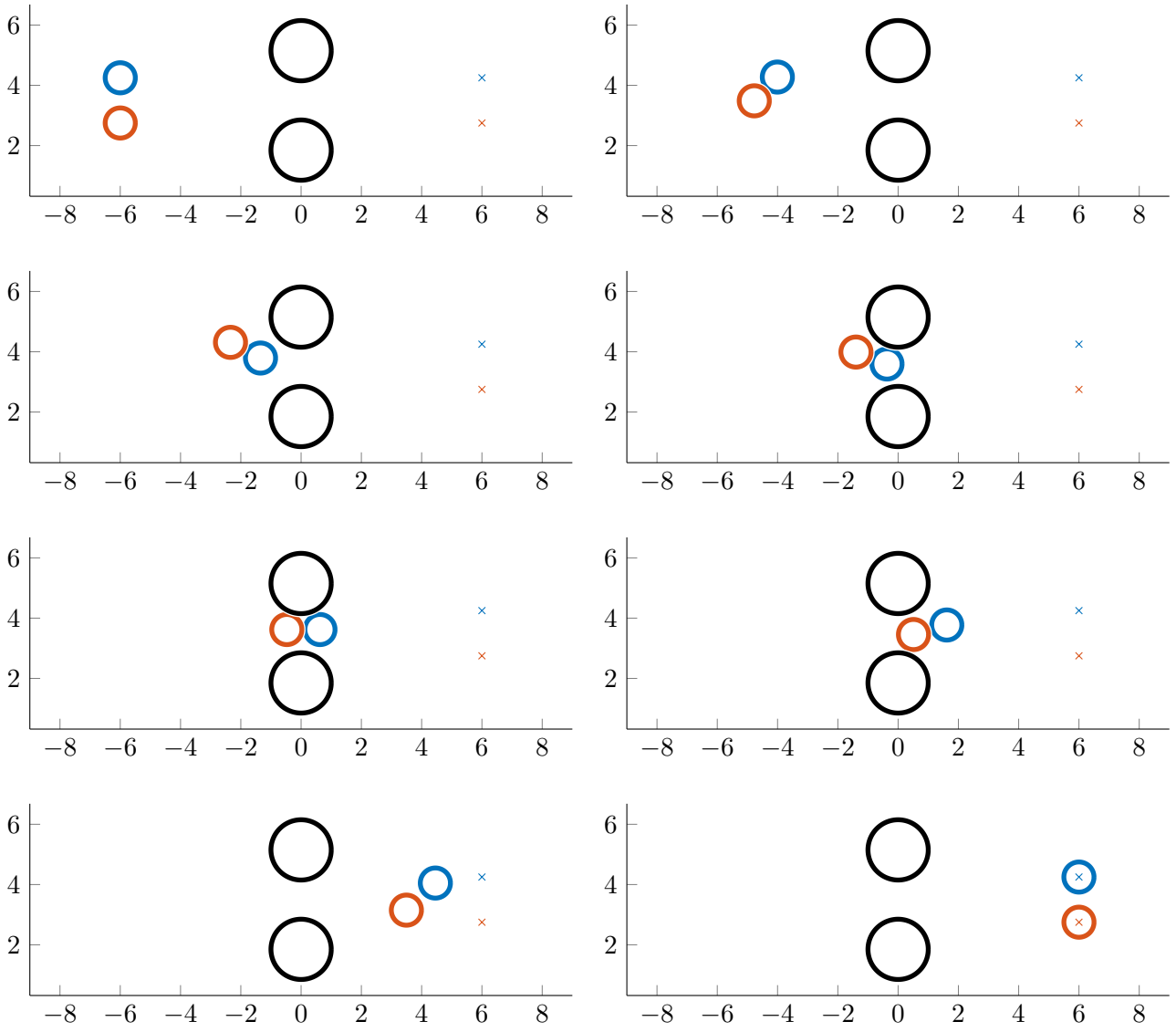

Figure B.8: The trajectories of the two agents in the $x - y$ plane.

B.2.2 State errors

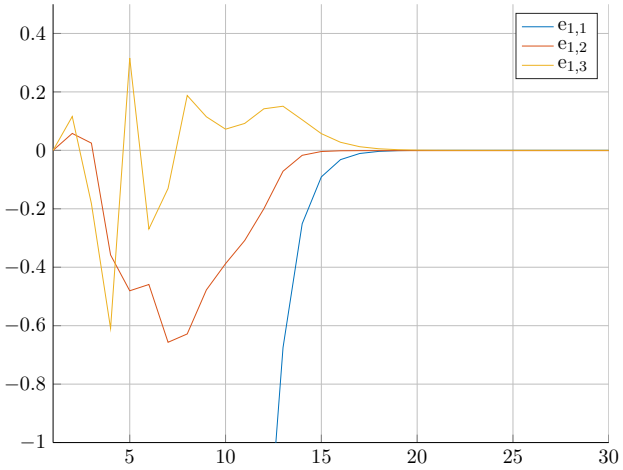

Figure B.9: The evolution of the error states of agent 1 over time.

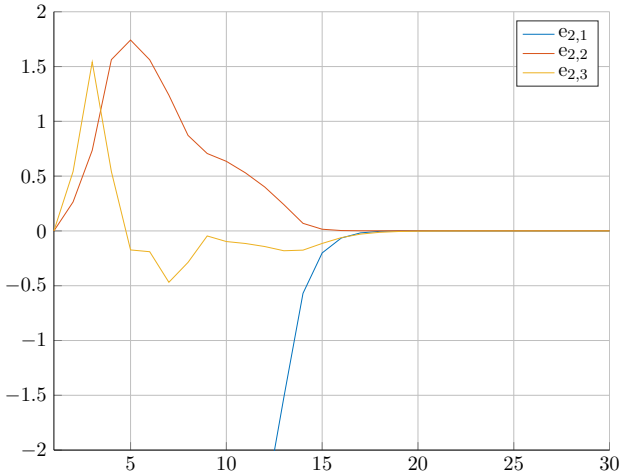

Figure B.10: The evolution of the error states of agent 2 over time.

B.2.3 Distances between actors

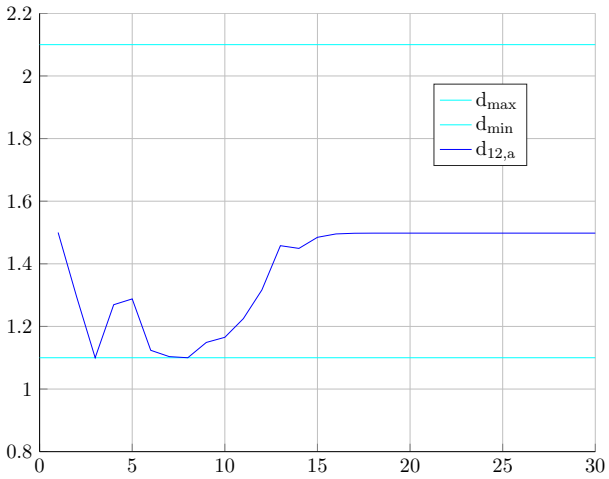

Figure B.11: The distance between the two agents over time. The maximum allowed distance has a value of 2.1 and the minimum allowed distance a value of 1.1.

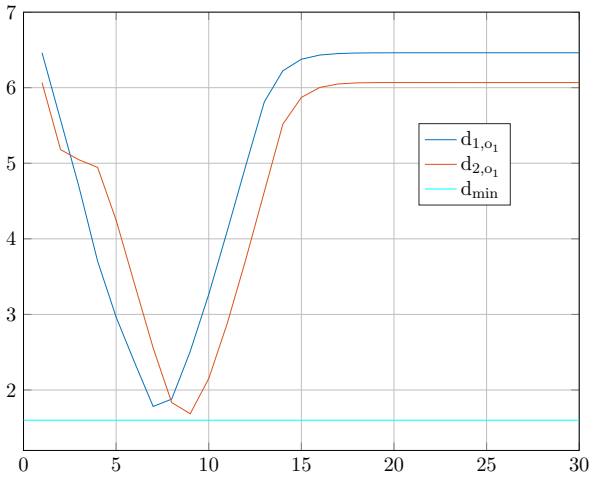

Figure B.12: The distance between each agent and obstacle 1 over time. The minimum allowed distance has a value of 1.6.

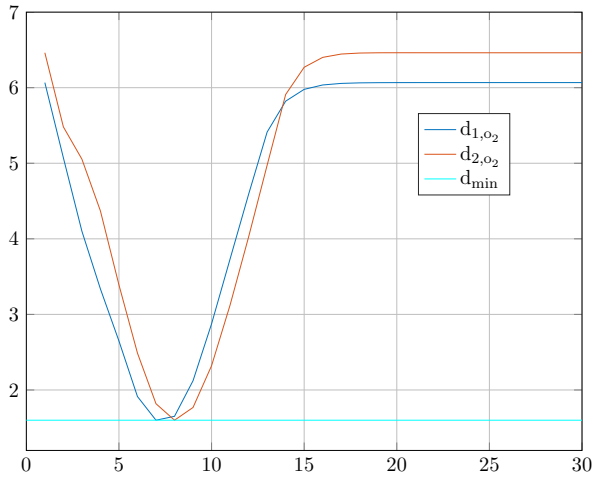

Figure B.13: The distance between each agent and obstacle 2 over time. The minimum allowed distance has a value of 1.6.

B.2.4 Input signals

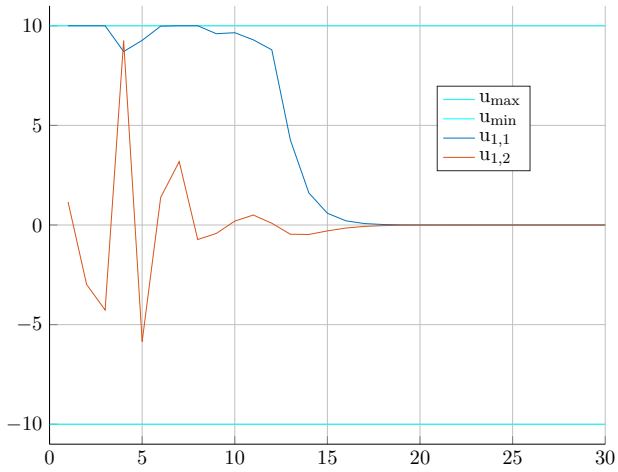

Figure B.14: The inputs signals directing agent 1 over time. Their value is constrained between −10 and 10.

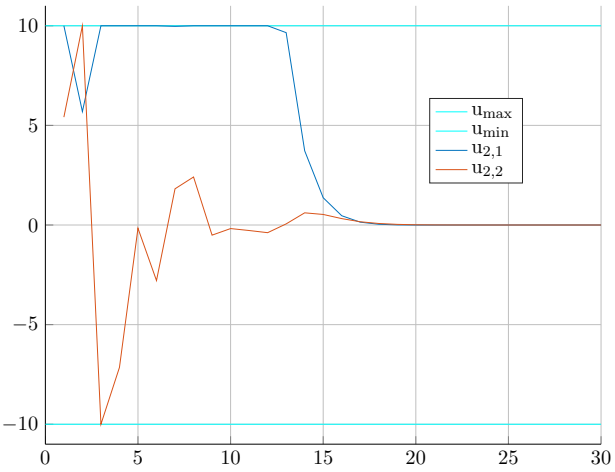

Figure B.15: The inputs signals directing agent 2 over time. Their value is constrained between −10 and 10.

B.3 Test case three: three agents − one obstacle

In this case the initial configurations of the three agents are $\mathbf{z}_1 = [-6, 3.5, 0]^\top$, $\mathbf{z}_2 = [-6, 2.3, 0]^\top$ and $\mathbf{z}_3 = [-6, 4.7, 0]^\top$. Their desired configurations in steady-state are $\mathbf{z}_{1,des} = [6, 3.5, 0]^\top$, $\mathbf{z}_{2,des} = [6, 2.3, 0]^\top$ and $\mathbf{z}_{3,des} = [6, 4.7, 0]^\top$. Obstacle o_1 is placed between the two

at $[0, 3.5]^\top$. The penalty matrices $\boldsymbol{Q}$, $\boldsymbol{R}$, $\boldsymbol{P}$ were set to $\boldsymbol{Q} = 0.5(I_3 + \dagger_3)$, $\boldsymbol{R} = 0.005I_2$ and $\boldsymbol{P} = 0.5I_3$, where $\dagger_N$ is a $N \times N$ matrix whose elements are chosen at random between the values 0.0 and 1.0.

In subsection 4.3.1, frames of the evolution of the trajectories of the three agents are depicted. Subsections 4.3.2 and 4.3.4 illustrate the evolution of the error states and the input signals of the three agents respectively. Subsection 4.3.3 features the figures relating to the evolution of the distance between the three agents along with that between them and the obstacle.

B.3.1 Trajectories in 2D

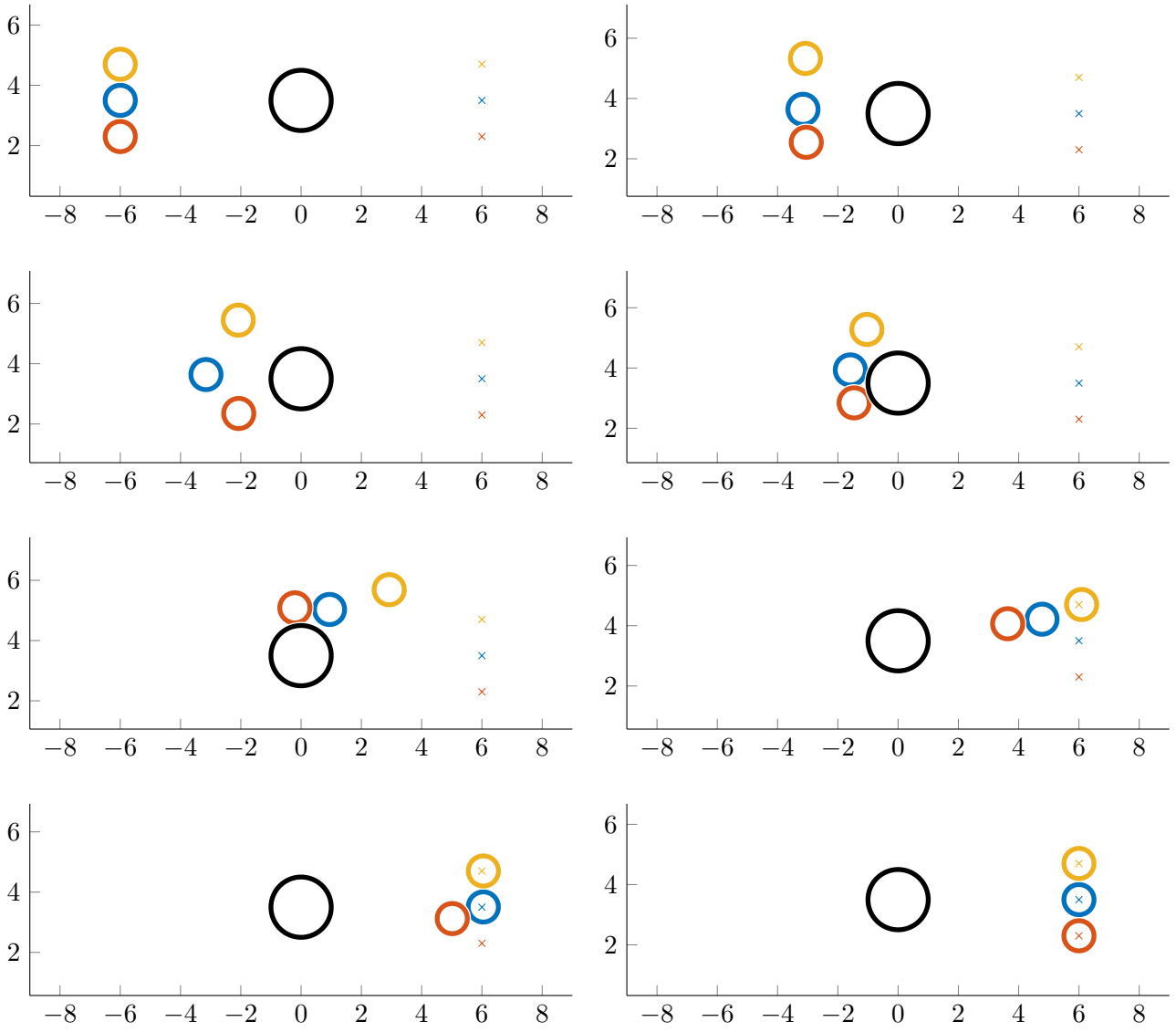

Figure B.16: The trajectories of the three agents in the $x - y$ plane.

B.3.2 State errors

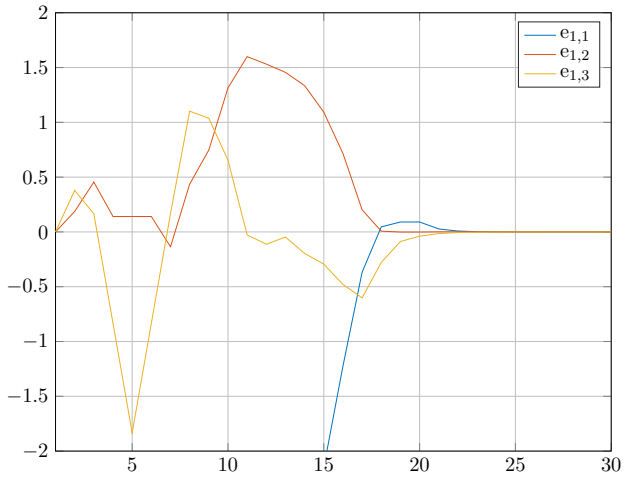

Figure B.17: The evolution of the error states of agent 1 over time.

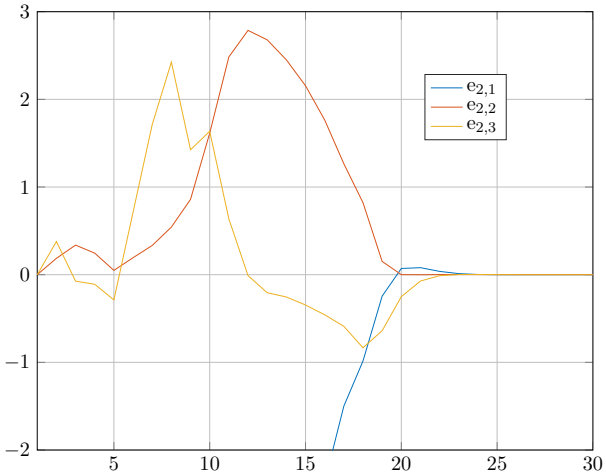

Figure B.18: The evolution of the error states of agent 2 over time.

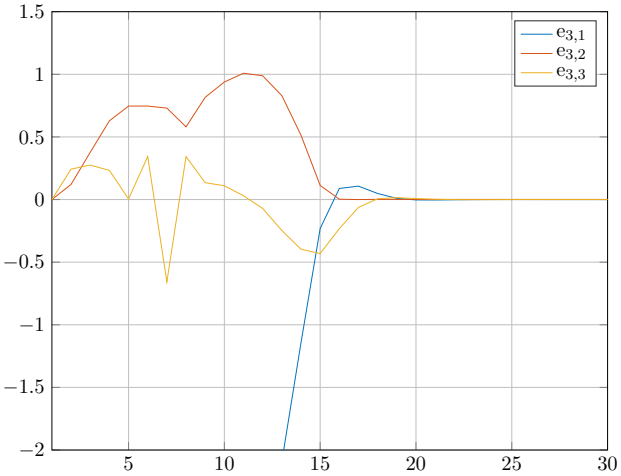

Figure B.19: The evolution of the error states of agent 3 over time.

B.3.3 Distances between actors

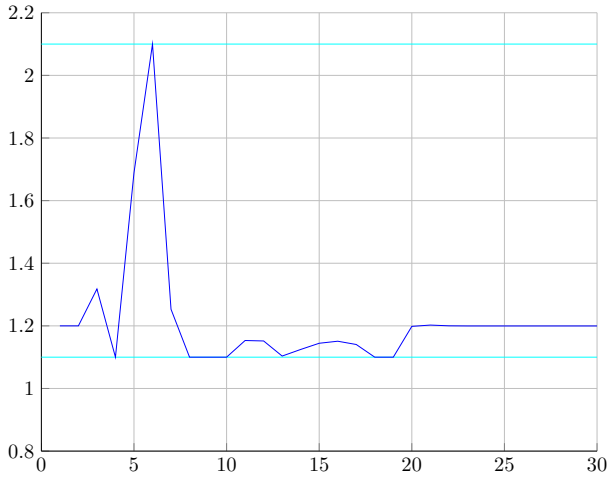

Figure B.20: The distance between agents 1 and 2 over time. The maximum allowed distance has a value of 2.1 and the minimum allowed distance a value of 1.1.

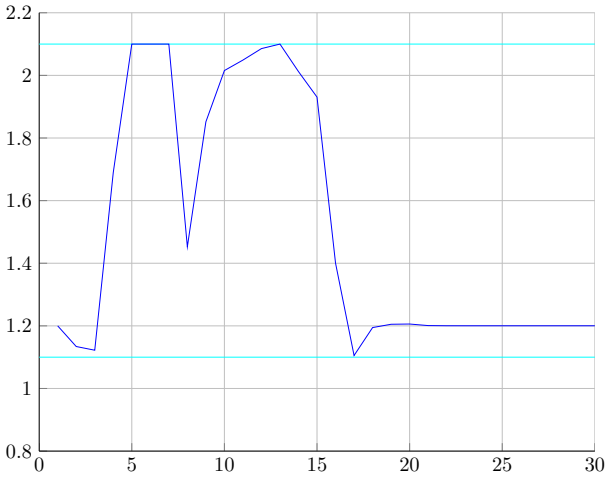

Figure B.21: The distance between agents 1 and 3 over time. The maximum allowed distance has a value of 2.1 and the minimum allowed distance a value of 1.1.

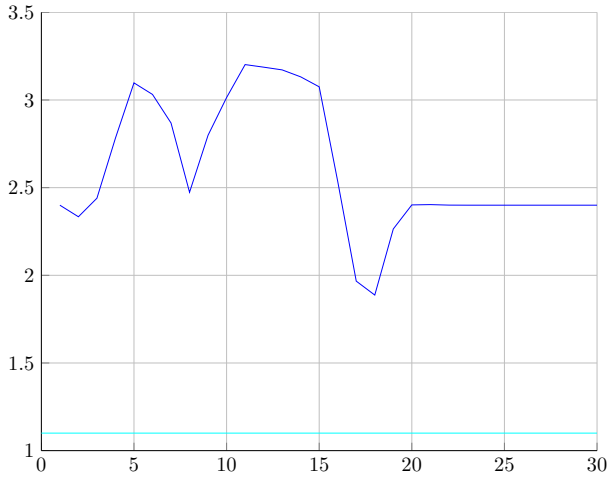

Figure B.22: The distance between agents 2 and 3 over time. The minimum allowed distance a value of 1.1.

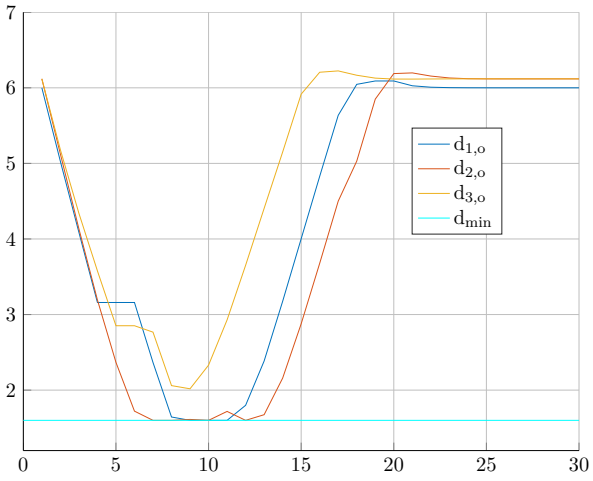

Figure B.23: The distance between each agent and the obstacle over time. The minimum allowed distance has a value of 1.6.

B.3.4 Input signals

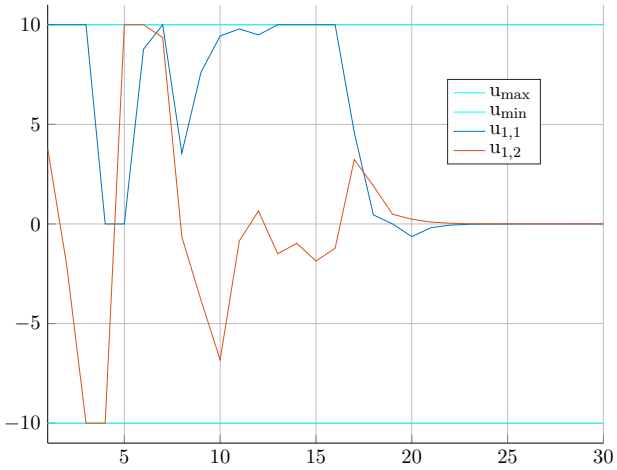

Figure B.24: The inputs signals directing agent 1 over time. Their value is constrained between −10 and 10.

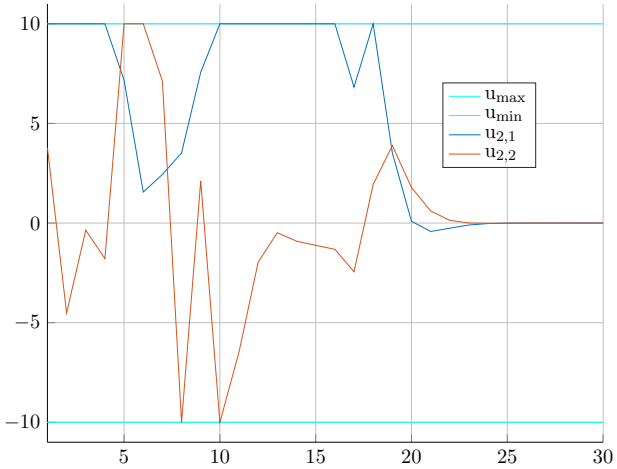

Figure B.25: The inputs signals directing agent 2 over time. Their value is constrained between −10 and 10.

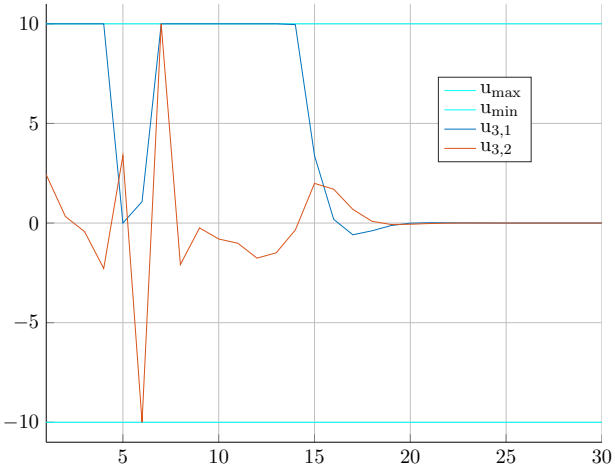

Figure B.26: The inputs signals directing agent 3 over time. Their value is constrained between −10 and 10.

B.4 Test case four: three agents – two obstacles

In this case the initial configurations of the three agents are $\mathbf{z}_1 = [-6, 3.5, 0]^\top$, $\mathbf{z}_2 = [-6, 2.3, 0]^\top$ and $\mathbf{z}_3 = [-6, 4.7, 0]^\top$. Their desired configurations in steady-state are $\mathbf{z}_{1,des} = [6, 3.5, 0]^\top$, $\mathbf{z}_{2,des} = [6, 2.3, 0]^\top$ and $\mathbf{z}_{3,des} = [6, 4.7, 0]^\top$. Obstacles o_1 and o_2 are placed

between the two at $[0, 2.0]^\top$ and $[0, 5.5]^\top$ respcetively. The penalty matrices $\boldsymbol{Q}$, $\boldsymbol{R}$, $\boldsymbol{P}$ were set to $\boldsymbol{Q} = 0.5(I_3 + 0.05\dagger_3)$, $\boldsymbol{R} = 0.005I_2$ and $\boldsymbol{P} = 0.5(I_3 + 0.05\dagger_3)$, where $\dagger_N$ is a $N \times N$ matrix whose elements are chosen at random between the values 0.0 and 1.0.

In subsection 4.4.1, frames of the evolution of the trajectories of the three agents are depicted. Subsections 4.4.2 and 4.4.4 illustrate the evolution of the error states and the input signals of the three agents respectively. Subsection 4.4.3 features the figures relating to the evolution of the distance between the three agents along with that between them and the two obstacles.

B.4.1 Trajectories in 2D

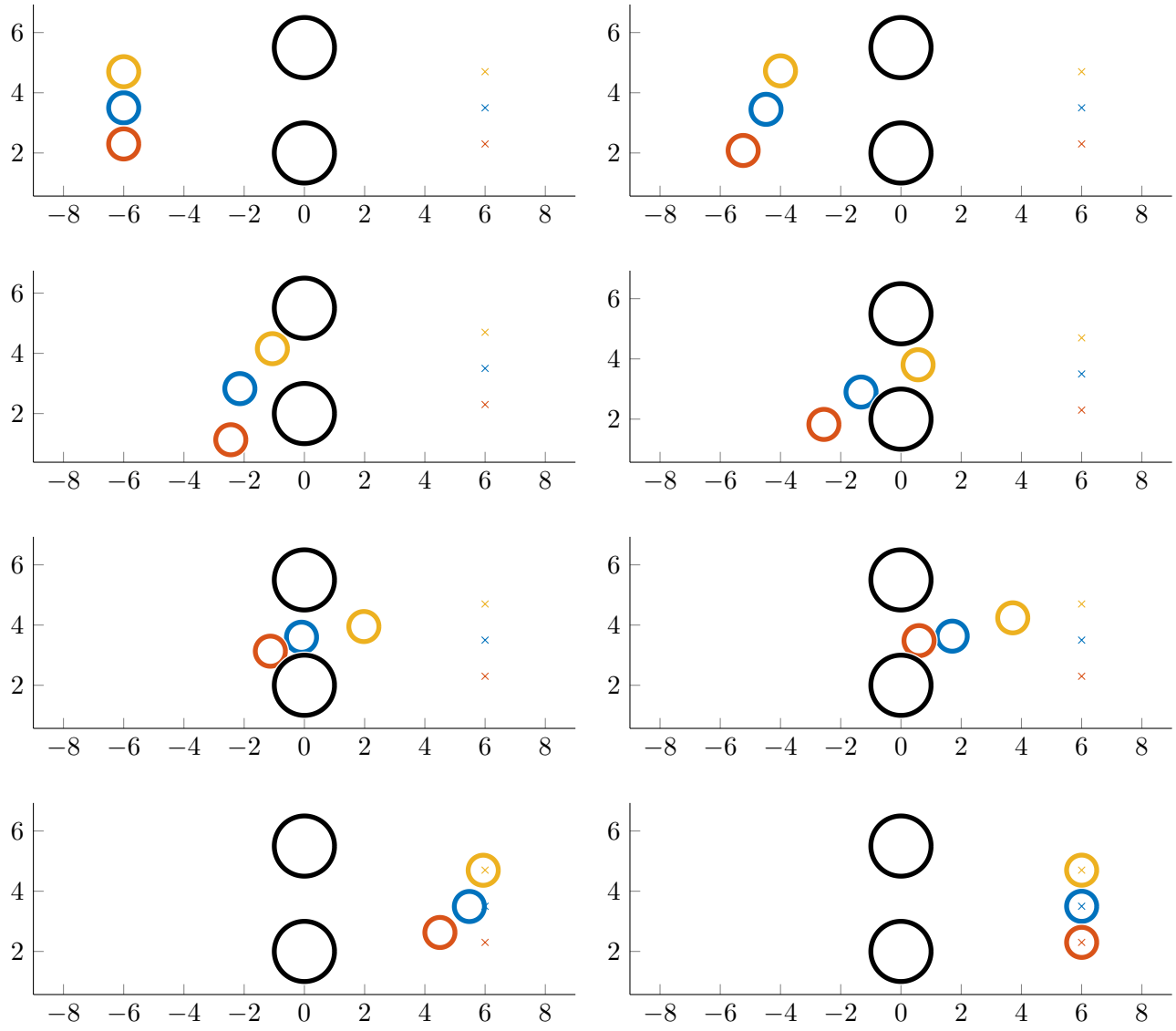

Figure B.27: The trajectories of the three agents in the $x - y$ plane.

B.4.2 State errors

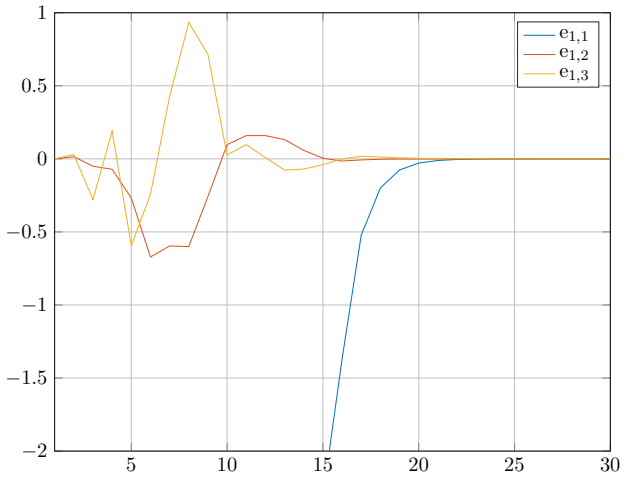

Figure B.28: The evolution of the error states of agent 1 over time.

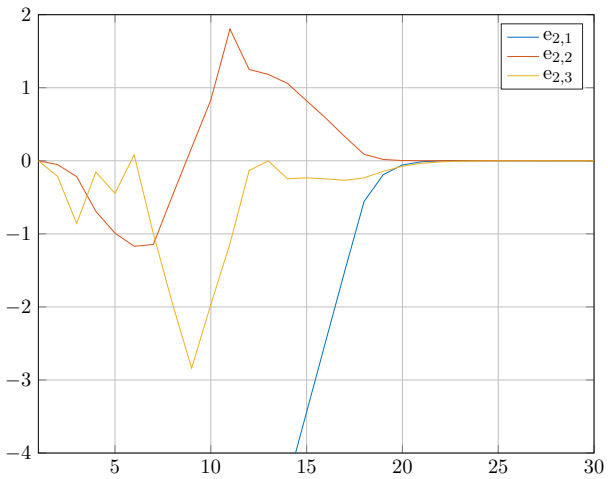

Figure B.29: The evolution of the error states of agent 2 over time.

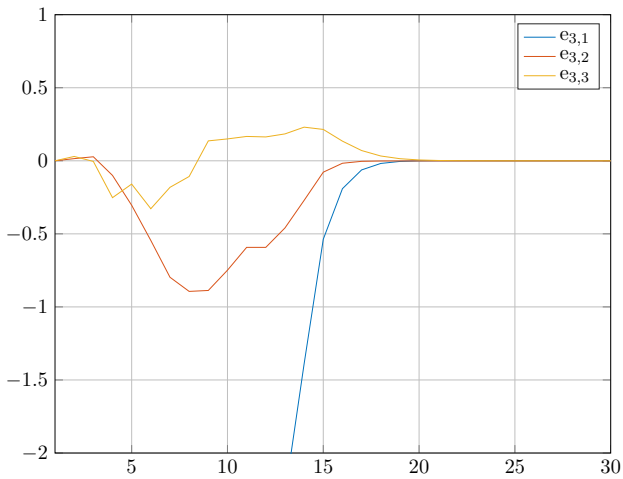

Figure B.30: The evolution of the error states of agent 3 over time.

B.4.3 Distances between actors

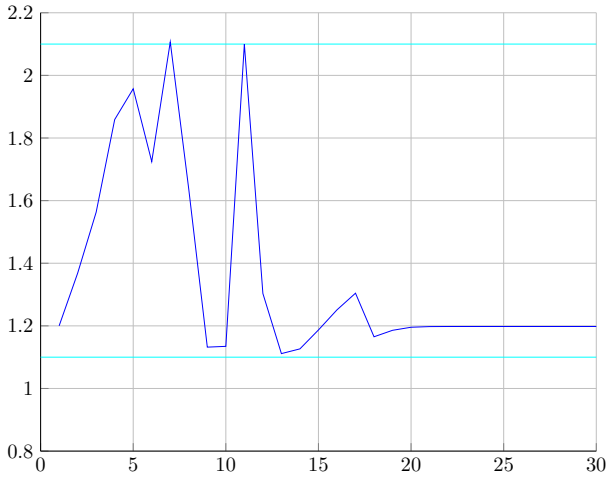

Figure B.31: The distance between agents 1 and 2 over time. The maximum allowed distance has a value of 2.1 and the minimum allowed distance a value of 1.1.

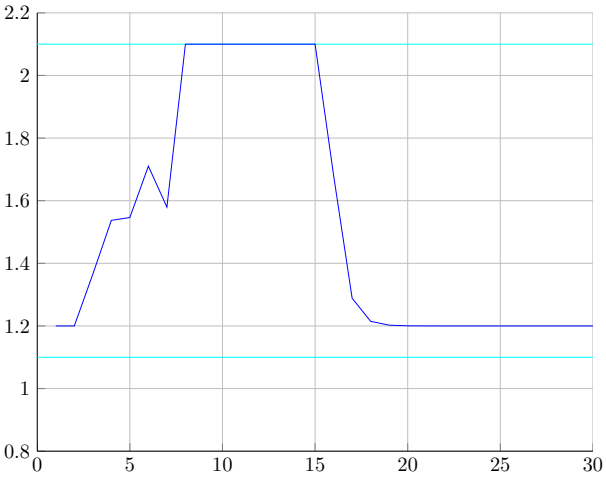

Figure B.32: The distance between agents 1 and 3 over time. The maximum allowed distance has a value of 2.1 and the minimum allowed distance a value of 1.1.

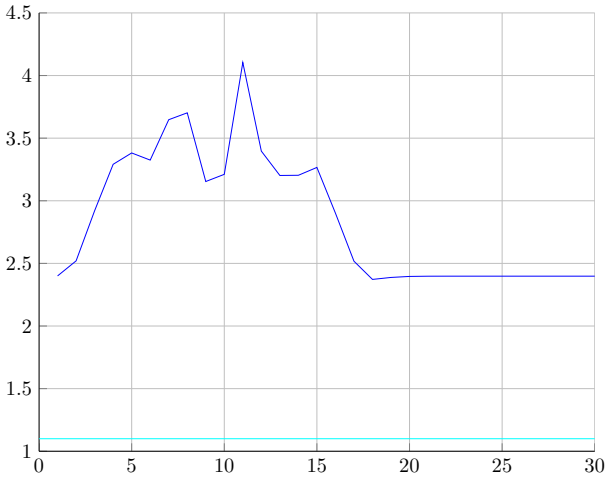

Figure B.33: The distance between agents 2 and 3 over time. The minimum allowed distance a value of 1.1.

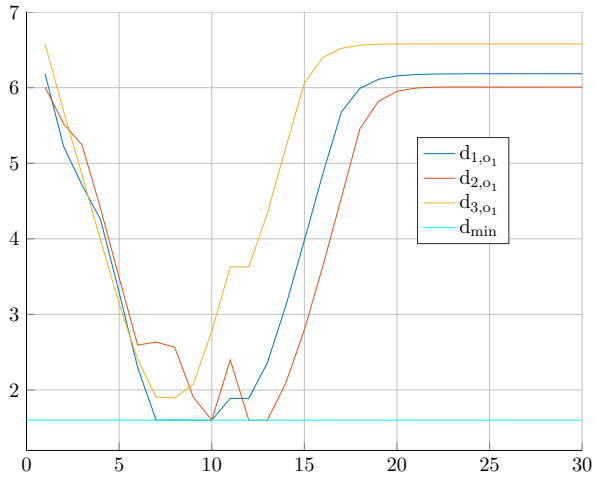

Figure B.34: The distance between each agent and obstacle 1 over time. The minimum allowed distance has a value of 1.6.

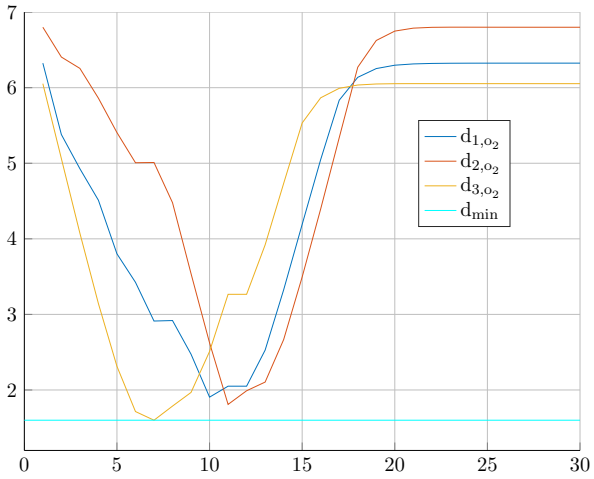

Figure B.35: The distance between each agent and obstacle 2 over time. The minimum allowed distance has a value of 1.6.

B.4.4 Input signals

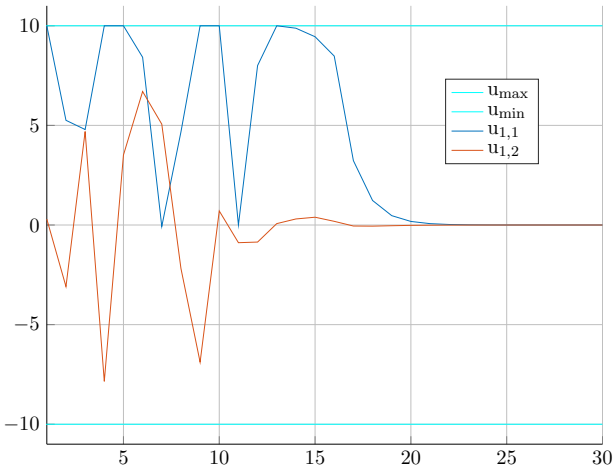

Figure B.36: The inputs signals directing agent 1 over time. Their value is constrained between −10 and 10.

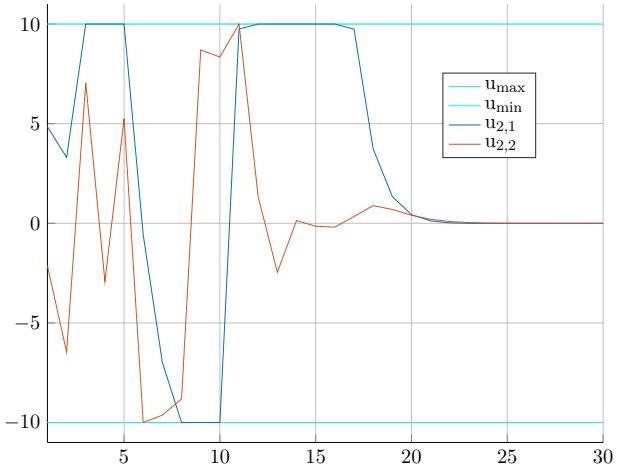

Figure B.37: The inputs signals directing agent 2 over time. Their value is constrained between −10 and 10.

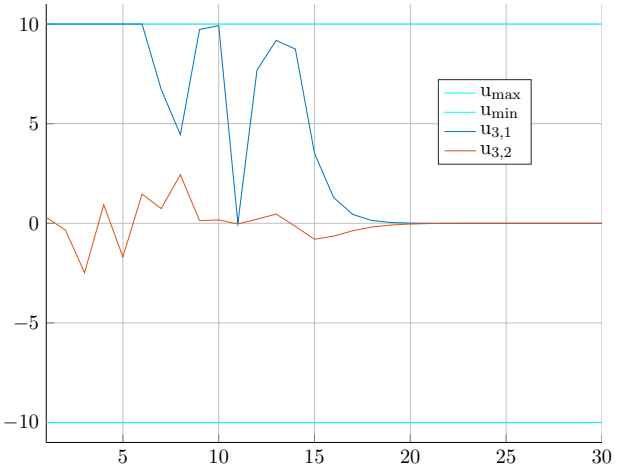

Figure B.38: The inputs signals directing agent 3 over time. Their value is constrained between −10 and 10.

C

Simulation figures – disturbances present

C.1 Test case one: two agents – one obstacle

C.1.1 State errors

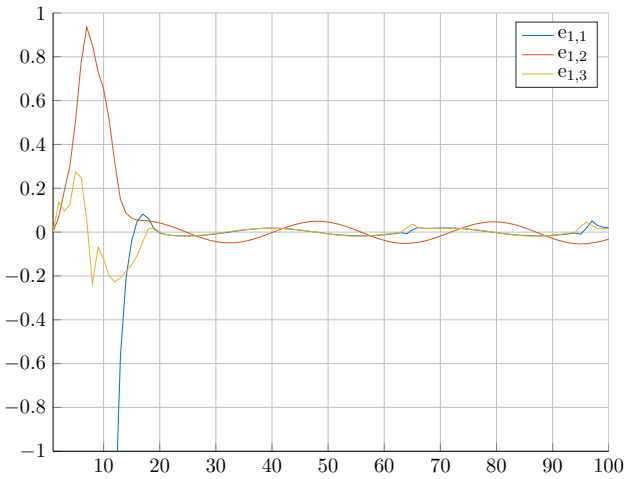

Figure C.1

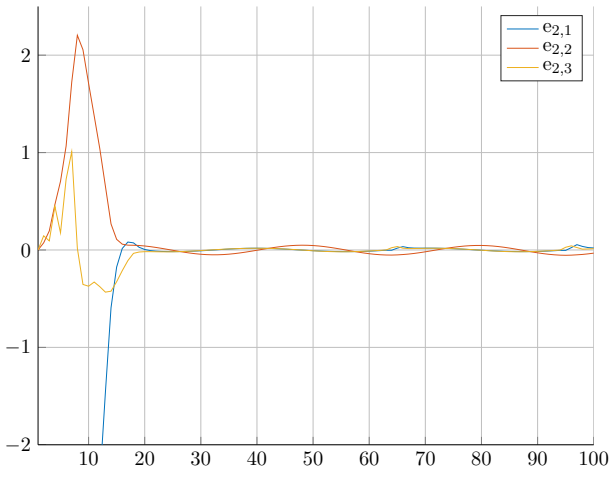

Figure C.2

C.1.2 Distances between actors

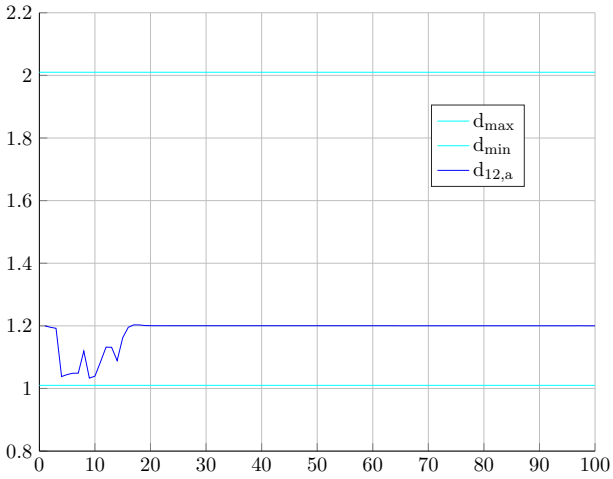

Figure C.3

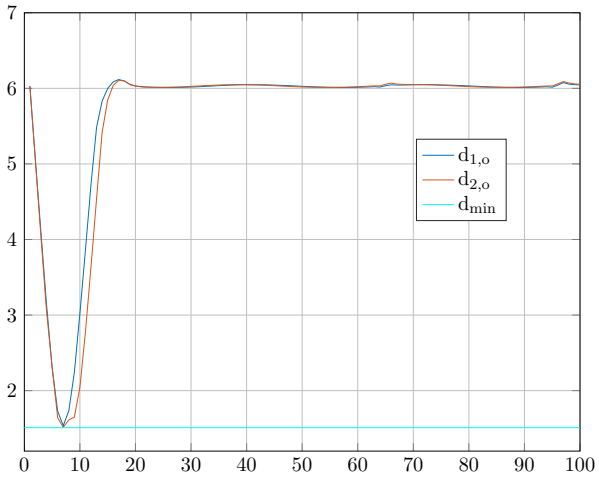

Figure C.4

C.1.3 Input signals

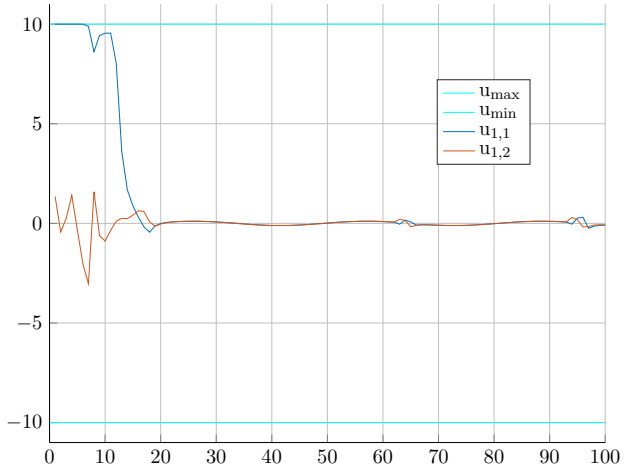

Figure C.5

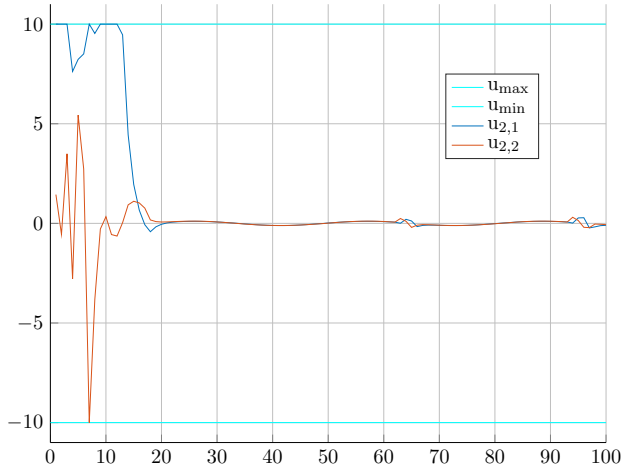

Figure C.6

C.1.4 Energy of the system

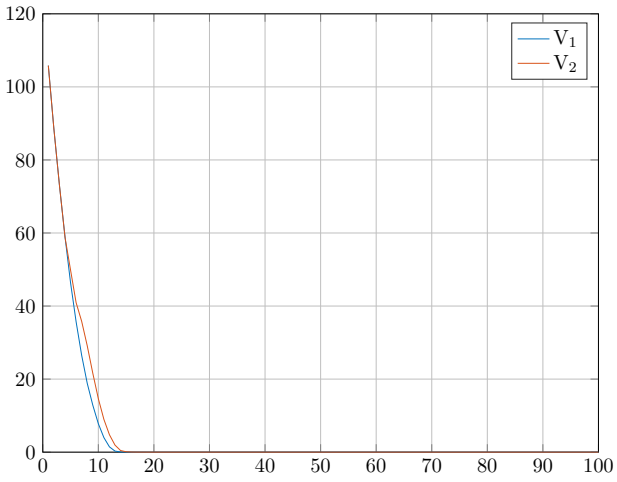

Figure C.7

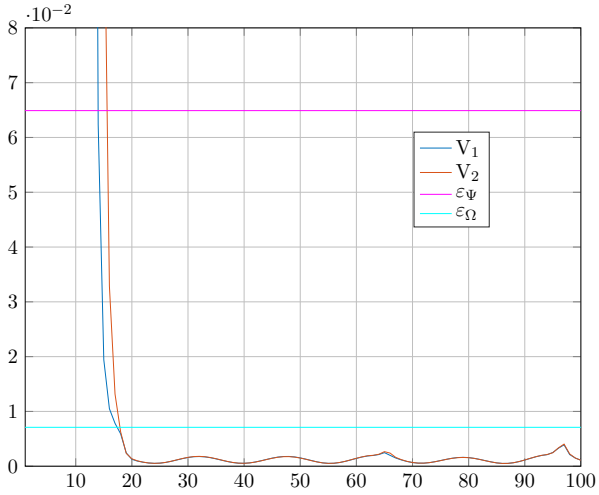

Figure C.8

C.2 Test case two: two agents – two obstacles

CHANGE

In this case, the initial configurations of the two agents are $\mathbf{z}_1 = [-6, 3.5, 0]^\top$ and $\mathbf{z}_2 = [-6, 2.3, 0]^\top$. Their desired configurations in steady-state are $\mathbf{z}_{1,des} = [6, 3.5, 0]^\top$ and $\mathbf{z}_{2,des} = [6, 2.3, 0]^\top$. The obstacle is placed between the two, at $[0, 2.9]^\top$. The time-horizon length was set to $T_p = 0.5$ sec. The penalty matrices $\boldsymbol{Q}$, $\boldsymbol{R}$, $\boldsymbol{P}$ were set to $\boldsymbol{Q} = 0.5(I_3 + 0.1\dagger_3)$, $\boldsymbol{R} = 0.005I_2$ and $\boldsymbol{P} = 0.5I_3$, where $\dagger_N$ is a $N \times N$ matrix whose elements are chosen at random between the values 0.0 and 1.0.

Trajectory, errors, etc (intro)

C.2.1 Trajectories in 2D

C.2.2 State errors

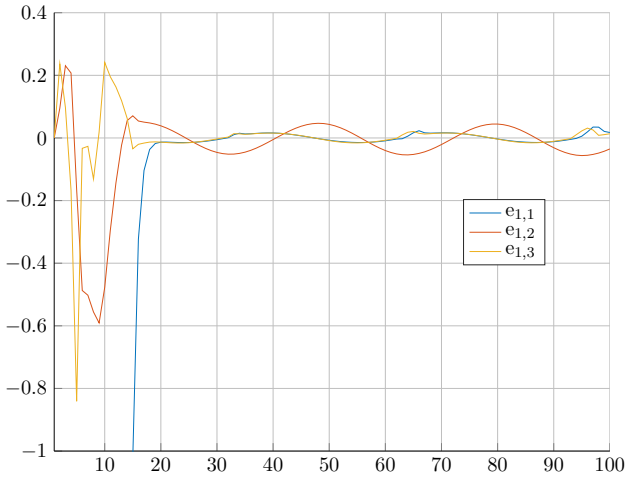

Figure C.9

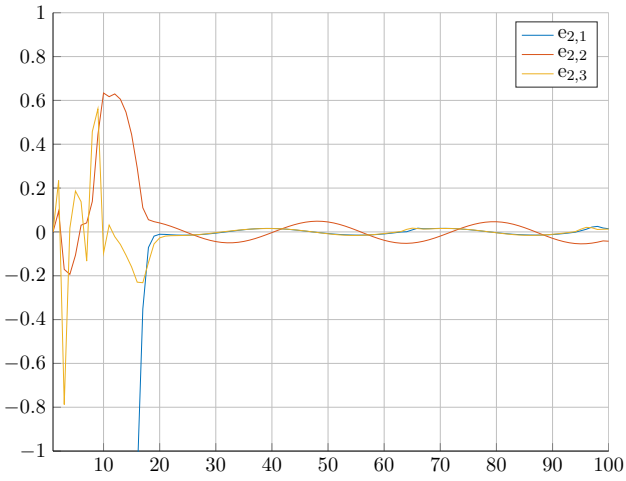

Figure C.10

C.2.3 Distances between actors

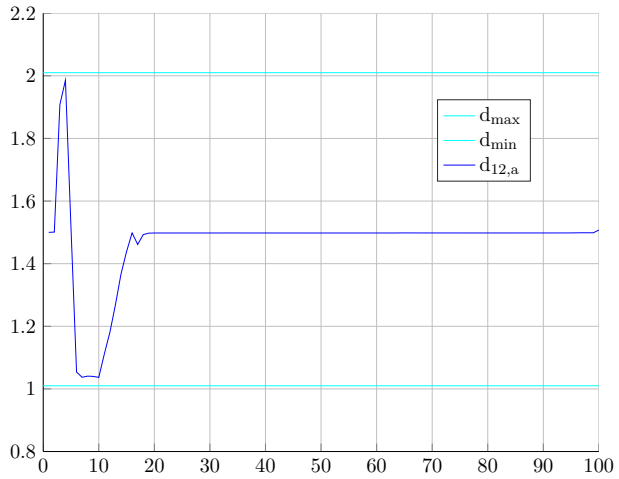

Figure C.11

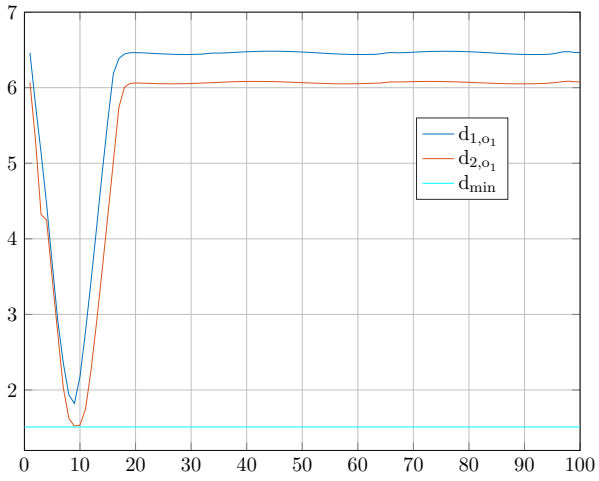

Figure C.12

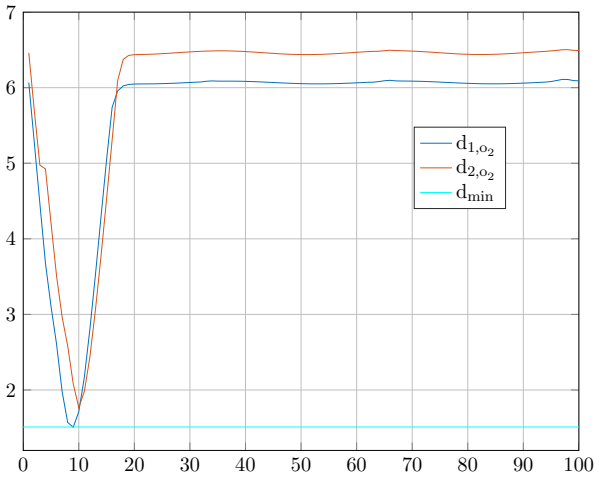

Figure C.13

C.2.4 Input signals

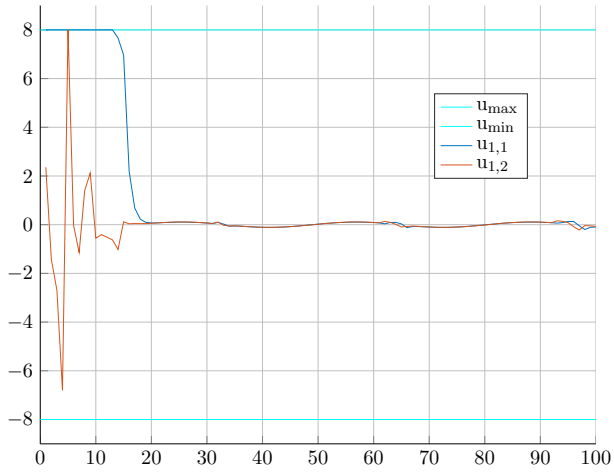

Figure C.14

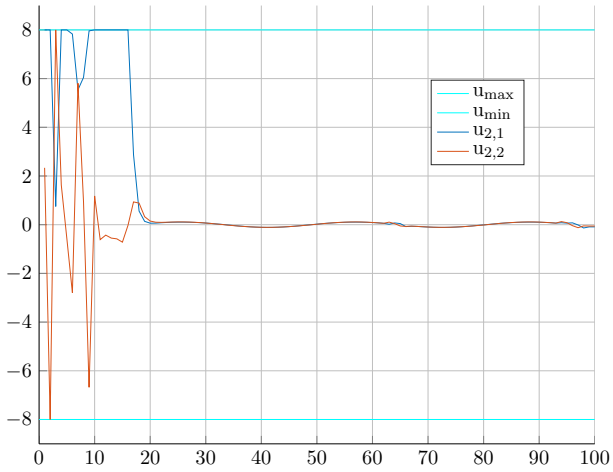

Figure C.15

C.2.5 Energy of the system

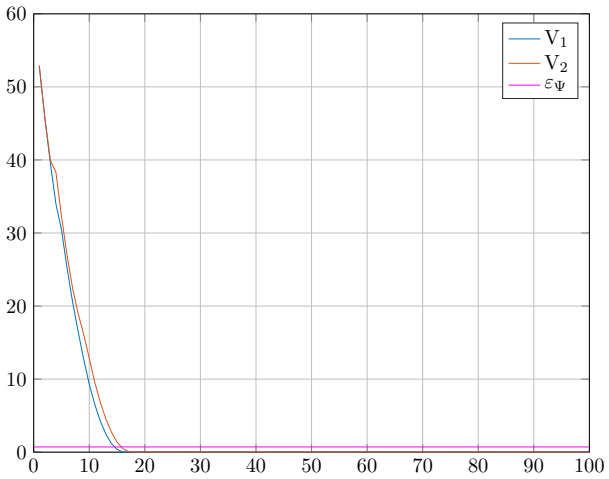

Figure C.16

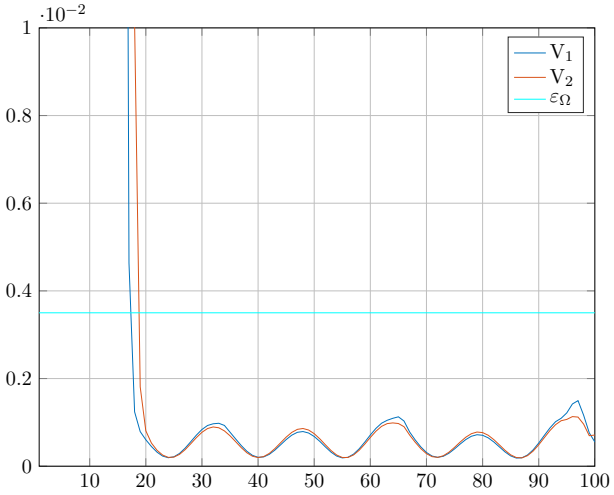

Figure C.17

C.3 Test case three: three agents – one obstacle

CHANGE

In this case, the initial configurations of the two agents are $\mathbf{z}_1 =$ and $\mathbf{z}_2 =$. Their desired configurations in steady-state are $\mathbf{z}_{1,des} =$ and $\mathbf{z}_{2,des} =$. The obstacle is placed between the two, at $[0, 2.9]^\top$. The time-horizon length was set to $T_p = 0.5$ sec. The penalty matrices $\boldsymbol{Q}$, $\boldsymbol{R}$, $\boldsymbol{P}$ were set to $\boldsymbol{Q} = 0.5(I_3 + 0.1\dagger_3)$, $\boldsymbol{R} = 0.005I_2$ and $\boldsymbol{P} = 0.5I_3$, where $\dagger_N$ is a $N \times N$ matrix whose elements are chosen at random between the values 0.0 and 1.0.

Trajectory, errors, etc (intro)

C.3.1 Trajectories in 2D

C.3.2 State errors

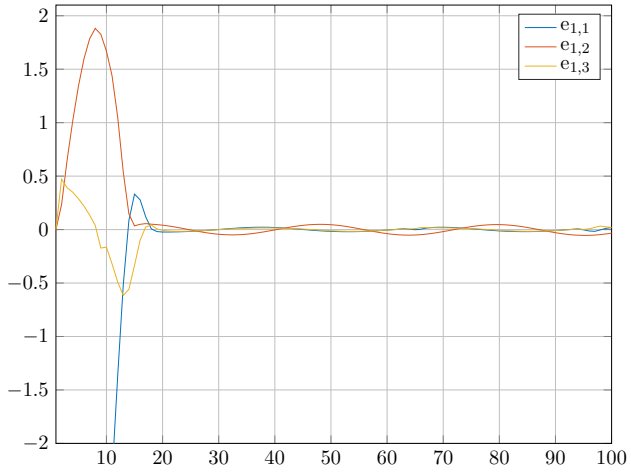

Figure C.18

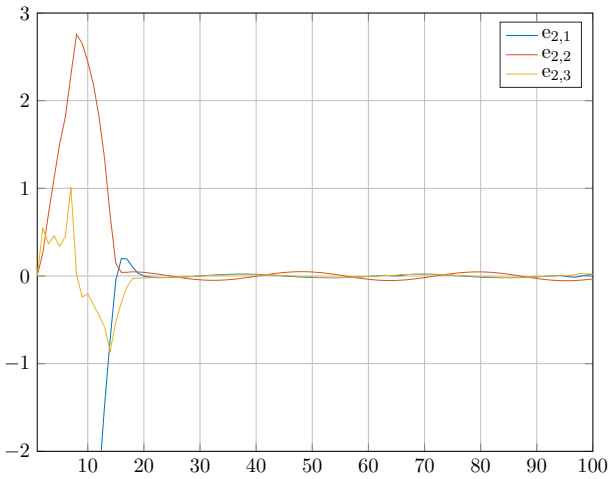

Figure C.19

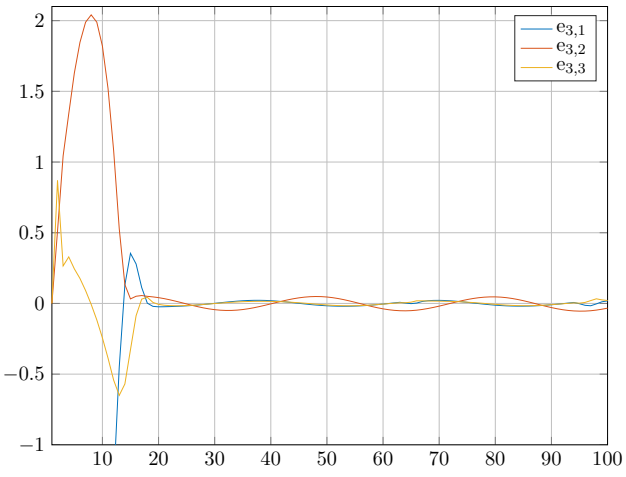

Figure C.20

C.3.3 Distances between actors

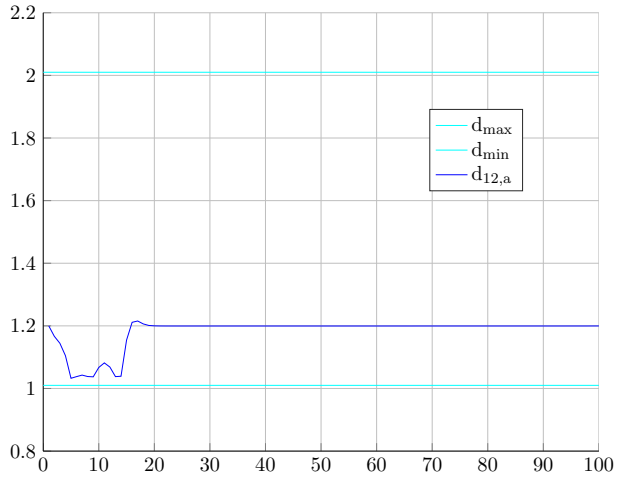

Figure C.21

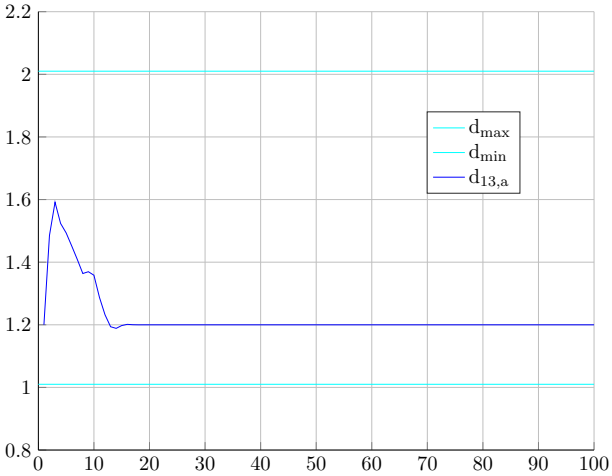

Figure C.22

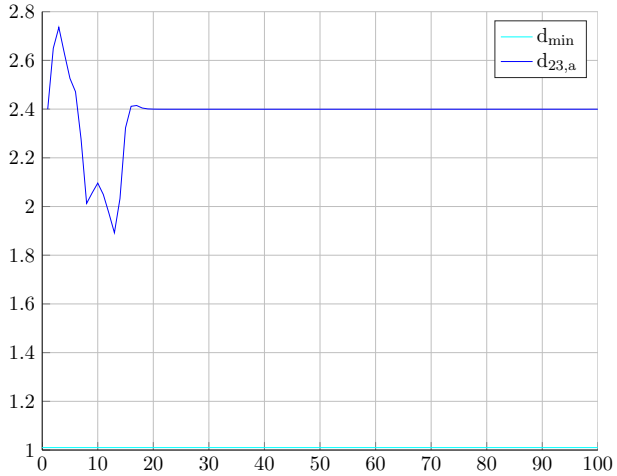

Figure C.23

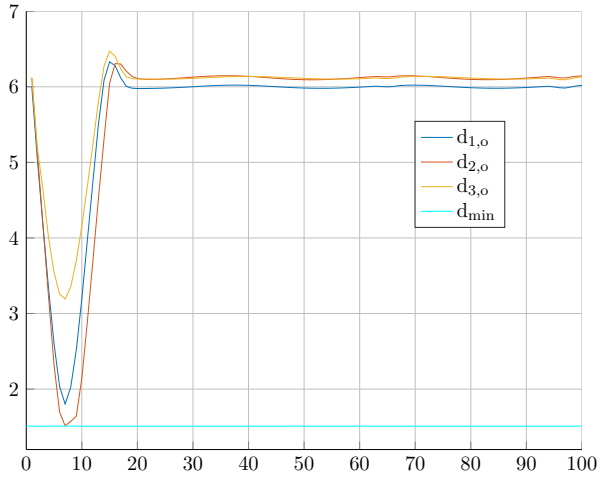

Figure C.24

C.3.4 Input signals

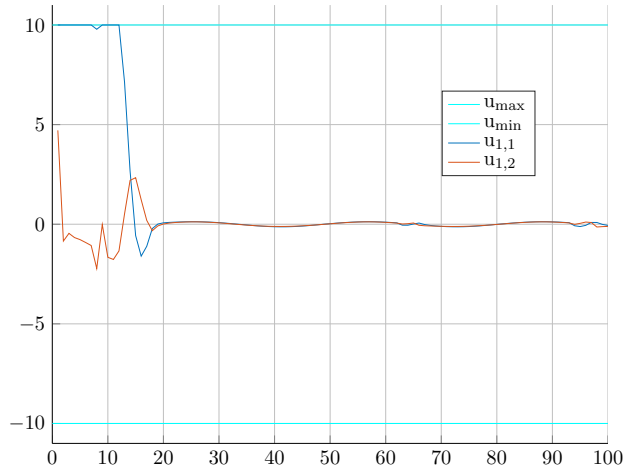

Figure C.25

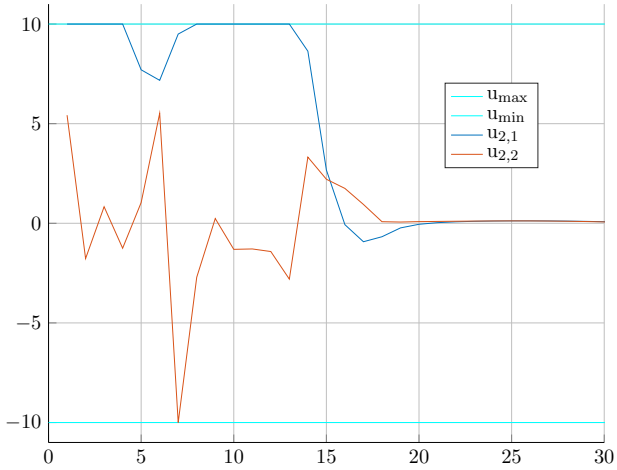

Figure C.26

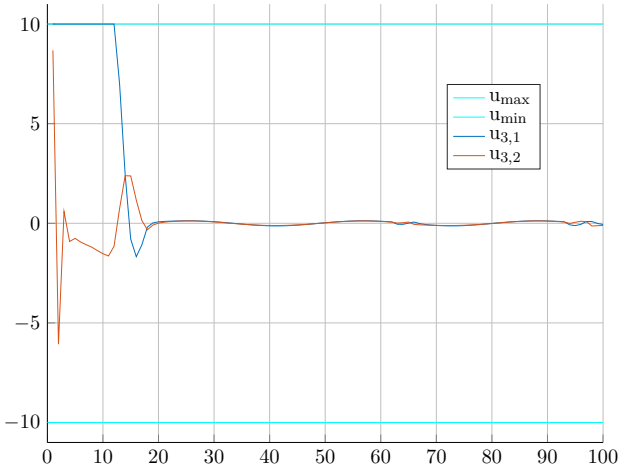

Figure C.27

C.3.5 Energy of the system

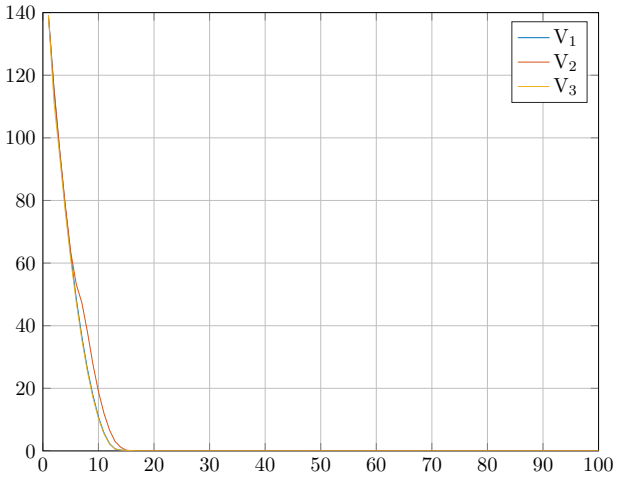

Figure C.28

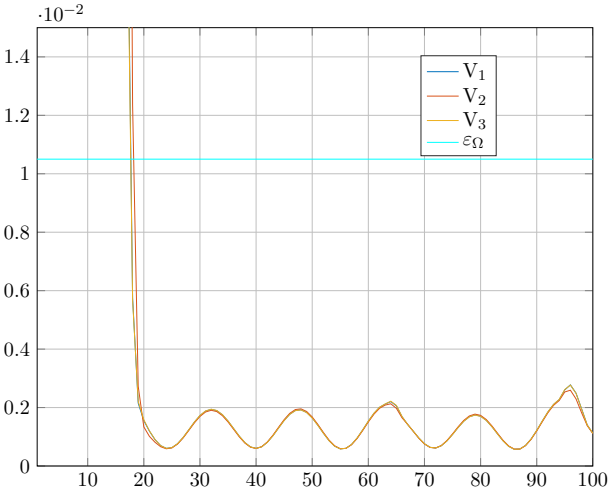

Figure C.29

C.4 Test case four: three agents – two obstacles

CHANGE

In this case, the initial configurations of the two agents are $\mathbf{z}_1 =$ and $\mathbf{z}_2 =$. Their desired configurations in steady-state are $\mathbf{z}_{1,des} =$ and $\mathbf{z}_{2,des} =$. The obstacle is placed between the two, at $[0, 2.9]^\top$. The time-horizon length was set to $T_p = 0.5$ sec. The penalty matrices $\boldsymbol{Q}$, $\boldsymbol{R}$, $\boldsymbol{P}$ were set to $\boldsymbol{Q} = 0.5(I_3 + 0.1\dagger_3)$, $\boldsymbol{R} = 0.005I_2$ and $\boldsymbol{P} = 0.5I_3$, where $\dagger_N$ is a $N \times N$ matrix whose elements are chosen at random between the values 0.0 and 1.0.

Trajectory, errors, etc (intro)

C.4.1 Trajectories in 2D

C.4.2 State errors

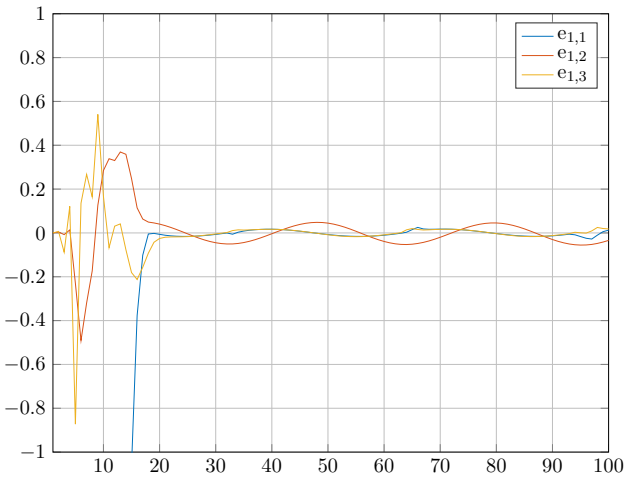

Figure C.30

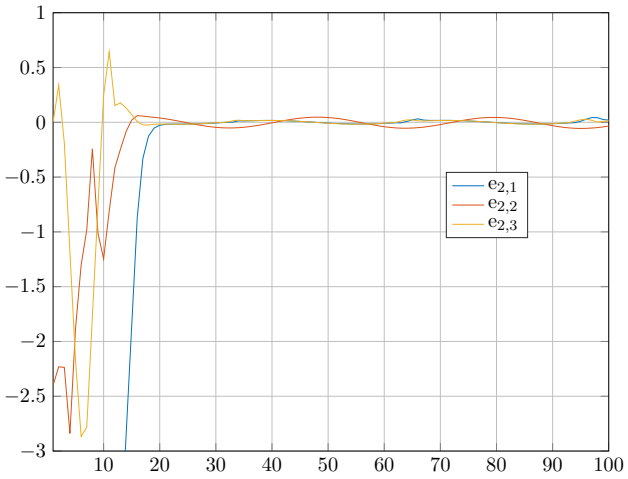

Figure C.31

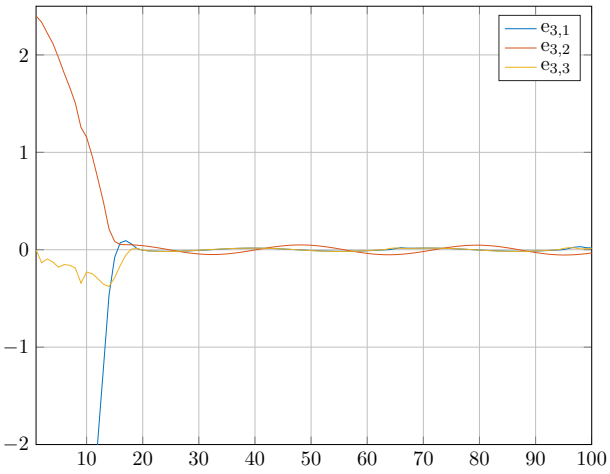

Figure C.32

C.4.3 Distances between actors

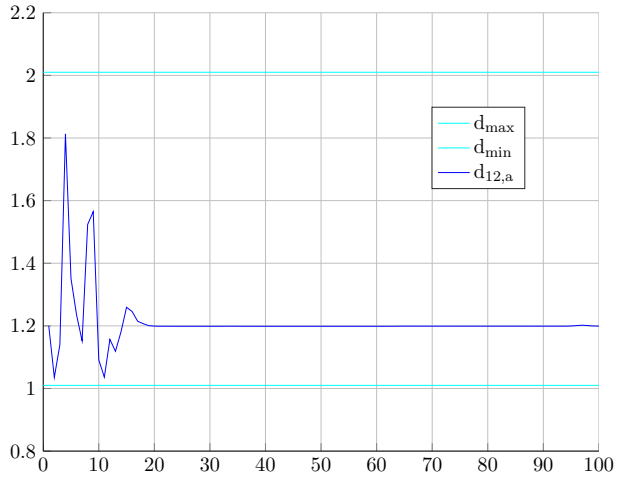

Figure C.33

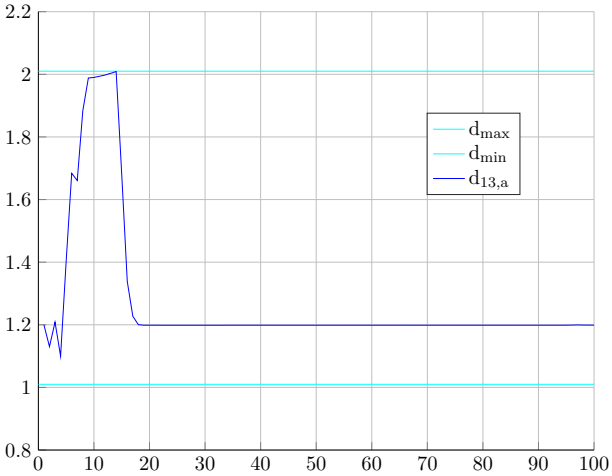

Figure C.34

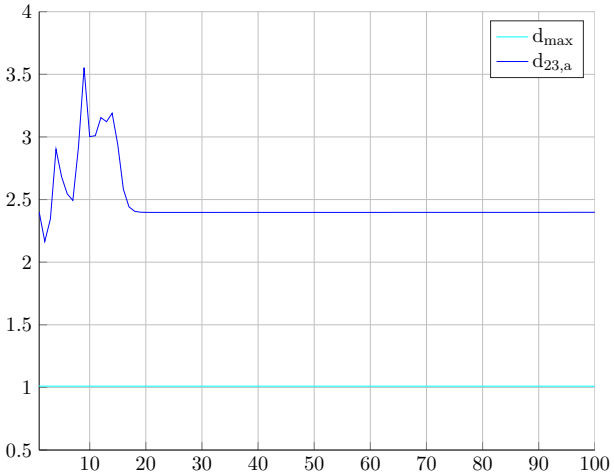

Figure C.35

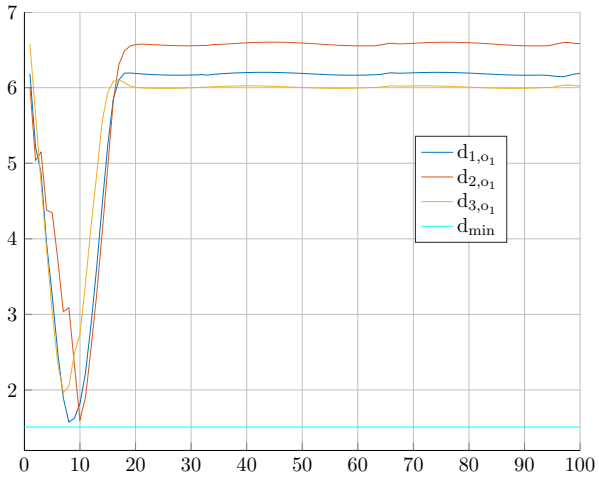

Figure C.36

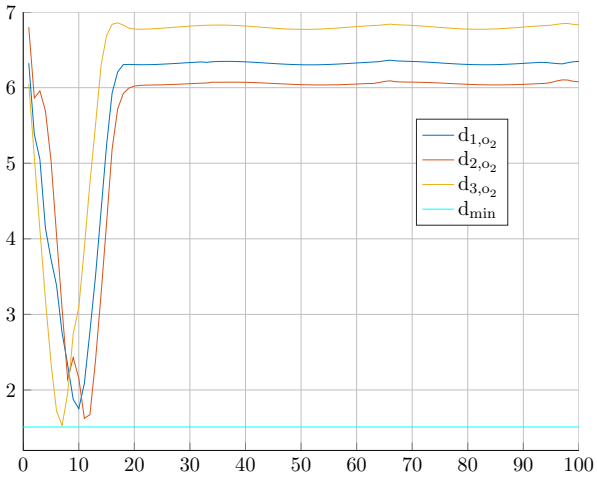

Figure C.37

C.4.4 Input signals

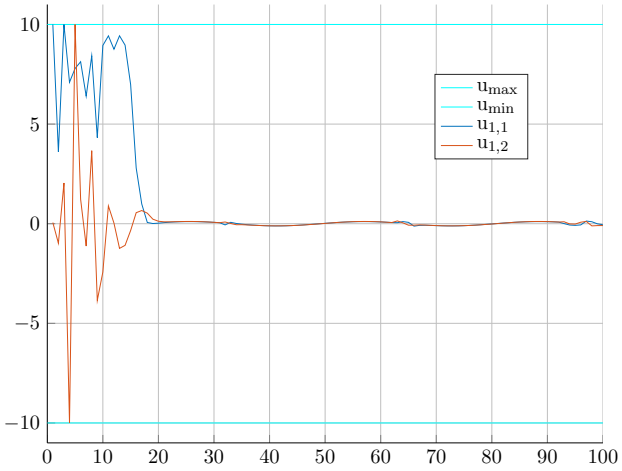

Figure C.38

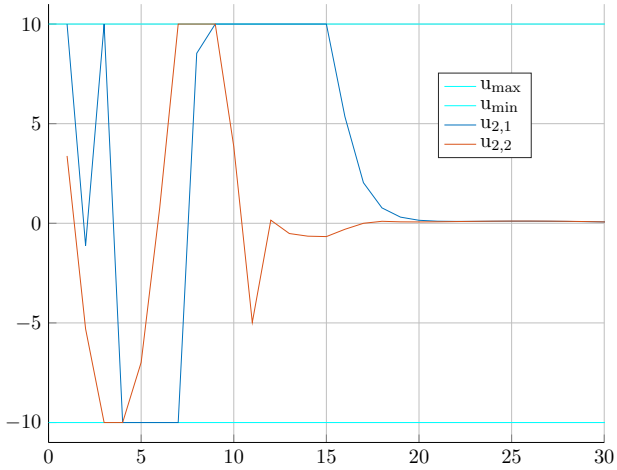

Figure C.39

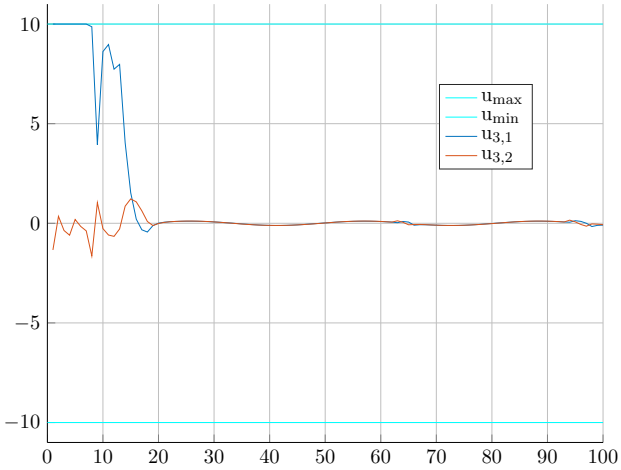

Figure C.40

C.4.5 Energy of the system

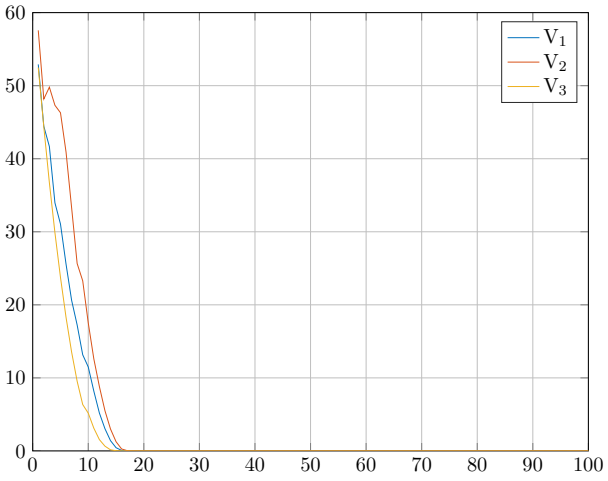

Figure C.41

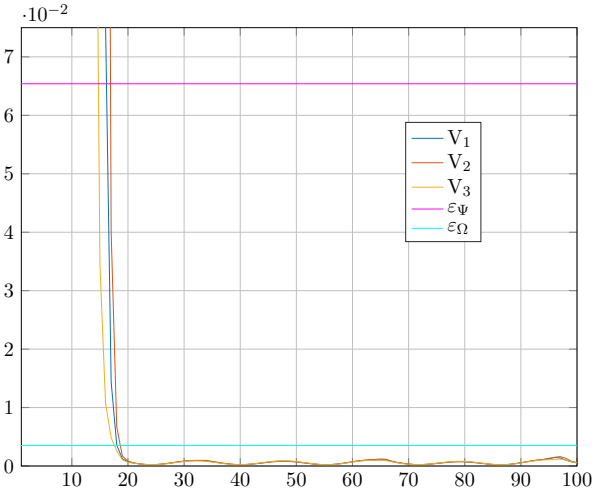

Figure C.42

Bibliography

[1] H. Khalil, *Noninear Systems.* Prentice-Hall, New Jersey, 1996.

[2] F. A. C. C. Fontes, L. Magni, and E. Gyurkovics, *Sampled-Data Model Predictive Control for Nonlinear Time-Varying Systems: Stability and Robustness*, pp. 115–129. Berlin, Heidelberg: Springer Berlin Heidelberg, 2007.

[3] H. Márquez, *Nonlinear Control Systems: Analysis and Design.* Wiley, 2003.

[4] D. L. Marruedo, T. Alamo, and E. F. Camacho, "Input-to-state stable mpc for constrained discrete-time nonlinear systems with bounded additive uncertainties," in *Proceedings of the 41st IEEE Conference on Decision and Control, 2002.*, vol. 4, pp. 4619–4624 vol.4, Dec 2002.

[5] L. Magni, D. M. Raimondo, and R. Scattolini, "Input-to-state stability for nonlinear model predictive control," in *Proceedings of the 45th IEEE Conference on Decision and Control*, pp. 4836–4841, Dec 2006.

[6] I. Kolmanovsky and E. G. Gilbert, "Theory and computation of disturbance invariant sets for discrete-time linear systems," *Mathematical Problems in Engineering*, vol. 4, no. 4, pp. 317–367, 1998.

[7] R. Schneider, *Minkowski addition*, pp. 139–207. Encyclopedia of Mathematics and its Applications, Cambridge University Press, 2013.